PACE Postlaunch Airborne eXperiment (PACE-PAX)

Draft as of January 20, 2022

Kirk D. Knobelspiesse, Brian Cairns, Ivona Cetinić, Susanne Craig, Bryan A. Franz, Meng Gao, Amir Ibrahim, Antonio Mannino, Andrew M. Sayer, P. Jeremy Werdell

Goddard Space Flight Center
Greenbelt, Maryland

National Aeronautics and Space Administration

1 INTRODUCTION

1.1 Purpose

The NASA Plankton, Aerosol, Cloud, ocean Ecosystem (PACE) mission is designed to observe the global ocean and atmosphere and provide extended data records of ocean ecology, biogeochemistry, atmospheric aerosols and clouds. The primary instrument on PACE, the Ocean Color Instrument (OCI), is a UV-VIS-NIR imaging spectrometer with additional discrete channels in the SWIR. Two other instruments have been contributed to PACE with more limited requirements. Both are multi-angle, polarization sensitive (MAP) imagers. The Hyper-Angular Rainbow Polarimeter 2 (HARP2) is a wide swath, four VIS-NIR channel sensor, while the Spectro-Polarimeter for Exploration (SPEXone) has a narrower swath but provides hyperspectral data.

PACE has requirements to produce ocean, aerosol, and cloud parameters from the OCI instrument. Additionally, a number of advanced science data products have been identified to be produced on a best-effort basis from all three instruments. An essential activity to these efforts is the validation of data product quality. This process involves the comparison of satellite data products to independently gathered observations of ocean, atmosphere, and land parameters. It also entails consideration of differences of scale, acquisition time, expectations of uncertainty, statistical sampling, and other matters by both satellite and independent measurements.

The overall plan for validation of PACE data is described in [document reference] "PACE Science Data Product Validation Plan" (hereafter referred to as the PVP). This document describes the required and advanced science data products to be validated, the PACE science data product Validation Program and its timeline, and the elements necessary for successful PACE validation. It also contains a brief section describing the requirements for field campaign(s) in support of PACE validation, while noting a forthcoming document describing these requirements in detail – this one.

This document describes the basis for, and requirements of, a PACE Postlaunch Airborne eXperiment (PACE-PAX). PACE-PAX will be conducted roughly 6 months to 1 year following the PACE launch and will deploy a variety of airborne and coordinated ground assets for the purpose of gathering validation and assessment data.

There are several reasons for augmenting PVP ground and ocean-based measurements with a dedicated airborne field campaign. These include, but are not limited to, the following.

1. **New products will be created from PACE observations**. They will need to be validated to assess quality and guide algorithm development. Dedicated field campaigns can make specific observations to this end. Furthermore, many of these products will be the result of multi-parameter algorithms, and retrieval capability for one geophysical property may depend on another, e.g., the accuracy of ocean chlorophyll-a pigment concentration products depend on the quantity and characteristics of atmospheric aerosols that are a part of atmospheric correction. Field campaigns that gather concurrent observations of multiple geophysical parameters enable a useful assessment of new products, particularly if they are made with airborne analogs of PACE instruments.

2. **Field campaigns that include airborne assets can provide for a different scale of observation** (spatial and temporal) than other validation sources, and a link between point measurements at the surface and the PACE orbital observatory.
3. **Airborne field campaigns can reposition assets within the spacecraft swath.** Due to its narrow swath, PACE's SPEXone instrument will have relatively few coincident observations with ground validation sites within the 3-year mission lifetime. Airborne assets can be directed to fly within the SPEXone swath during an overpass, adding many validation observations to an otherwise limited dataset.
4. **Airborne assets can validate PACE radiometric and polarimetric observations** prior to their use for retrieval of geophysical parameters.
5. **Remote sensing success depends on observation geometry, season, and time of day**, which can be directly targeted with field campaigns.
6. **Field campaigns can focus on specific systems, processes or phenomena** to verify they are properly accounted for in the satellite retrieval scheme**.**

The characteristics of PACE-PAX are described in this document, including a further discussion of how field campaign observations fit within the larger scope of PACE validation, what independent measurements are required, the logistical considerations for carrying out the mission, and the support required to properly measure, analyze, and archive the observed data.

1.2 PACE mission overview

The original definition of the PACE mission is included in *Responding to the Challenge of Climate and Environmental Change: NASA's Plan for Climate-Centric Architecture for Earth Observations and Applications from Space,* as a bridge mission to aerosol (particulate matter in the atmosphere), cloud, and ocean ecosystem observing mission(s) described in the National Research Council's 2007 Decadal Survey of Earth Science for NASA, NOAA and USGS, entitled *Earth Science and Applications from Space: National Imperatives for the Next Decade and Beyond.* As such, PACE will produce heritage products that provide continuity with existing climate and Earth system records, and also create new advanced products for emerging science questions related to the Earth's changing climate.

The PACE observatory includes three instruments. The Ocean Color Instrument (OCI) is a hyper-spectral scanning radiometric imager that will measure from the ultraviolet (UV) to shortwave infrared (SWIR) with a view-angle tilt to avoid ocean surface reflected sun glint. OCI is the primary instrument on PACE, and it is in development at the NASA Goddard Space Flight Center (GSFC). OCI will produce heritage ocean, aerosol and cloud products, and advanced products that take advantage of hyper-spectral and UV sensitivity. PACE will also include two contributed multi-angle polarimeters (MAP), instruments that maximize observed information with the use of multiple geometry measurements and determination of the polarization state of light. Developed at the University of Maryland, Baltimore County (UMBC), the Hyper-Angular Rainbow Polarimeter (HARP2) instrument is a wide swath imager intended for determination of cloud and aerosol optical parameters through the utilization of hyper-angle measurement capability. The Spectro- Polarimeter for Exploration (SPEXone) is a highly accurate (although narrow swath) hyperspectral MAP intended for the identification of detailed aerosol (and other) parameters. It is being developed by a consortium in the Netherlands that includes Airbus and the Netherlands

Institute for Space Research (SRON). Table 1 contains details on the measurement characteristics of each instrument.

Table 1 Instrument specifications for OCI, HARP2 and SPEXone. Recreated from Table 2 of Werdell et al., 2019. * The mission carries a goal of extending the shortest wavelength to 320nm. + There is a 2-day coverage when limited to solar and sensor viewing angles of 75˚ and 60˚, respectively.

	OCI	HARP2	SPEXone
UV-NIR range (bandwidth)	Continuous from 340 to 890nm* in 5-nm steps (5)	440, 550, 670 (10), and 870 (40) nm	Continuous from 385 to 770 nm in 2-4nm steps
SWIR range (bandwidth)	940 (45), 1,038 (75), 1,250 (30), 1,378 (15), 1,615 (75), 2,130 (50) and 2,260 (75) nm	None	None
Polarized bands	None	All	Continuous from 385 to 770 nm in 15-45nm steps
Number of viewing angles	Fore-aft instrument tilt of ±20˚ to avoid sun glint	10 for 440, 550 and 870 nm and 60 for 670 nm (spaced over 114˚)	5 (-57˚, -20˚, 0˚, 20˚, 57˚)
Swath width	±56.6˚ (2,663 km at 20˚ tilt)	±47˚ (1,556km at nadir)	±4˚ (100 km at nadir)
Global coverage	1-2+ days	2 days	~30 days
Ground pixel	1 km at nadir	3 km	2.5 km
Institution	GSFC	UMBC	SRON/Airbus

PACE will be launched into an ascending polar orbit at a nominal spacecraft altitude of 676.5 kilometers, with a local crossing time of 13:00 and inclination angle of 98°. Observations will cover the globe regularly, and the length of time required to observe the entire globe depends on the instrument swath. As shown with other instrument characteristics in Table 1, the wider swath OCI and HARP2 instruments require 1-2 days for global coverage, while the narrow swath SPEXone instrument will require roughly 30 days. For that instrument, overflights of fixed ground validation sites will be much less frequent.

PACE is classified as a Category 2 mission, per the criteria in NASA Procedural Requirement (NPR) 7120.5E, NASA Space Flight Program and Project Management Requirements. The mission classification is C according to NPR 8705.4B, Risk Classification for NASA Payloads. The scheduled launch date is in 2023.

1.3 Mission requirements for validation

The PACE Program Level Requirements Agreement (PLRA) and Mission Requirements Document (MRD) (see section 1.4) provide the requirements pertaining to the PACE Science Data Product Validation Program:

"Post-launch field validation work is required to evaluate the PACE science data products in Tables 1 and 2 within 12 months of commissioning. The PACE validation programs (provided by HQ PACE Science) shall include the following for the mission duration:

a) Shipboard and aircraft campaigns as required to collect the data products defined in Tables 1 and 2.

b) *Autonomous instrument systems that collect continuous records of any of the individual data products defined in Tables 1 and 2."*

Tables 1 and 2 referenced in this quote are replicated as Tables 2 and 3, respectively, in this document. These are the required data products to be produced by the PACE Project Science and Science Data Segments (SDS). Project Science is responsible for data product quality and must therefore validate by comparing to independent observations. In addition, NASA Headquarters (HQ) PACE Program Science competes both the PACE Science and Applications Team (SAT) and the PACE Validation Science Team (PVST) which contribute algorithms, data, insight and other guidance to Program Science and the SDS to ensure date quality.

The required products in Tables 2 and 3 must be validated within 12 months of PACE spacecraft commissioning. These required products are only for the OCI sensor, and, with some exceptions, can be considered 'Heritage,' that is, produced by previously launched missions. The MAP instruments (HARP2 and SPEXone) are contributed to the PACE mission with requirements limited to "do no harm" to the rest of the spacecraft, so there are no required products from those instruments. However, the full list of expected PACE products (Tables 4-10) represent new measurements and science that all three PACE sensors (OCI, HARP2, and SPEXone) may address. The science and algorithms supporting many of these products are in development by the SAT, Project Science, and instrument teams. An important aspect of this development is the validation of these new products. Some, but not all, can be validated using the resources called for in the PVP. The remainder require additional efforts and resources, as described in this document. Tables 4-10 represent an evolving list of products that are captured on the PACE website (https://pace.oceansciences.org/data_table.htm). The process by which algorithms are selected, tested, and implemented in the PACE SDS is described in the PACE Science Data Product Selection Plan (SDPSL).

Table 2 Required OCI ocean color data products. The requirements for ocean color products stated in Table 1 are defined for 50% or more of the observable deep ocean (depth>1000 m).

Data Product	Baseline Uncertainty
Water-leaving reflectances centered on (±2.5 nm) 350, 360, and 385 nm (15 nm bandwidth)	0.0057 or 20%
Water-leaving reflectances centered on (±2.5 nm) 412, 425, 443, 460, 475, 490, 510, 532, 555, and 583 (15 nm bandwidth)	0.0020 or 5%
Water-leaving reflectances centered on (±2.5 nm) 617, 640, 655, 665 678, and 710 (15 nm bandwidth, except for 10 nm bandwidth for 665 and 678 nm)	0.0007 or 10%
Ocean Color Data Products to be Derived from Water-leaving Reflectances	
Concentration of chlorophyll-a	
Diffuse attenuation coefficients 400-600 nm	
Phytoplankton absorption 400-600 nm	
Non-algal particle plus dissolved organic matter absorption 400-600 nm	
Particulate backscattering coefficient 400-600 nm	
Fluorescence line height	

Table 3. Required OCI aerosol and cloud data products. The requirements in this table are defined for 65% or more of the observable atmosphere. Each requirement is defined as the maximum of the absolute and relative values when both are provided. This table represents threshold aerosol and cloud data products, all of which can be produced by OCI alone.

Data Product	Range	Baseline Uncertainty
Total aerosol optical depth at 380 nm	0.0 to 5	0.06 or 40%
Total aerosol optical depth at 440, 500, 550 and 675 nm over land	0.0 to 5	0.06 or 20%
Total aerosol optical depth at 440, 500, 550 and 675 nm over oceans	0.0 to 5	0.04 or 15%
Fraction of visible aerosol optical depth from fine mode aerosols over oceans at 550 nm	0.0 to 1	±25%
Cloud layer detection for optical depth > 0.3	NA	40%
Cloud top pressure of opaque (optical depth > 3) clouds	100 to 1000 hPa	60 hPa
Optical thickness of liquid clouds	5 to 100	25%
Optical thickness of ice clouds	5 to 100	35%
Effective radius of liquid clouds	5 to 50 μm	25%
Effective radius of ice clouds	5 to 50 μm	35%
Atmospheric data products to be derived from the above		
Water path of liquid clouds		
Water path of ice clouds		

As previously mentioned, Tables 2 and 3 describe PACE required products from the OCI sensor. These are to be validated as described in the PVP, with additional assessment as described in this document. Table 4 lists the radiometric products that will be produced at top of atmosphere (TOA) from all three sensors. The "Level-1B" data format refers to calibrated data at TOA, while "Level-1C" is a data format for which all sensor observations are represented on a compatible, equal area grid (L1Cplan). The latter is especially important for multiangle observations by SPEXone and HARP2 and will serve as the starting point for algorithms that determine geophysical (Level-2) products using data from multiple sensors. For example, the proposed microphysical aerosol parameters from polarimetry algorithm (MAPP, Stamnes et al., 2018) will start with either SPEXone or HARP2 data at Level-1C and combine that with SWIR observations by OCI to retrieve coupled atmosphere and ocean optical parameters.

Table 4 Calibrated Radiometry and Polarimetry, as observed at sensor.

Product	Description and Use	Units	Availability	Status
Spectral top-of-atmosphere radiances from OCI	Spectral radiance observed at the top of the atmosphere.	W m^{-2} um^{-1} sr^{-1}	Level-1B at 1 km^2 at nadir, daily; Level-1C 5.2 km^2, daily	Standard product
Spectral top-of-atmosphere radiances and polarimetry from SPEXone	Spectral radiance and polarimetry observed at the top of the atmosphere, for all sensor viewing angles.	Various	Level-1B at TBD km^2, daily; Level-1C at 2.6 km^2, daily	Standard product
Spectral top-of-atmosphere radiances and	Spectral radiance and polarimetry observed at the top of the	Various	Level-1B at TBD km^2, daily; Level-	Standard product

polarimetry from HARP2	atmosphere, for all sensor viewing angles.		1C at TBD km^2, daily	

1.4 Related documentation

1. PACE Program Level Requirements Agreement (PLRA), PACE-SYS-REQ-0007
2. PACE Mission Requirements Document (MRD), PACE-SYS-REQ-0019
3. NASA Earth Science Data Systems (ESDS) Program Data and Information Policy, https://earthdata.nasa.gov/earth-science-data-systems-program/policies/data-information-policy
4. Pre-Aerosol, Clouds, and ocean Ecosystem (PACE) Mission Science Definition Team (SDT) Report, NASA/TM-2018-219027/Vol. 2 https://pace.oceansciences.org/docs/PACE_TM2018-219027_Vol_2.pdf
5. PACE Science Data Product Validation Plan (PVP), https://pace.oceansciences.org/docs/PACE_Validation_Plan_DRAFT_version_24March2020_posted.pdf
6. *Responding to the Challenge of Climate and Environmental Change: NASA's Plan for Climate-Centric Architecture for Earth Observations and Applications from Space* https://science.nasa.gov/earth-science/documents
7. *Earth Science and Applications from Space: National Imperatives for the Next Decade and Beyond* (2007) https://www.nap.edu/catalog/11820/earth-science-and-applications-from-space-national-imperatives-for-the
8. *Thriving on Our Changing Planet: A Decadal Strategy for Earth Observation from Space* (2017) https://www.nap.edu/catalog/25437/thriving-on-our-changing-planet-a-decadal-strategy-for-earth-observation-from-space
9. Pre-Aerosol, Clouds, and ocean Ecosystem (PACE) Science Data Product Selection Plan (SDPSL), NASA/TM-TM-2020-219027/Vol. 8 https://pace.oceansciences.org/docs/TM-20205007069-2020-219027-Vol.-8-PACE_vol8.pdf
10. The PACE Level 1c data format (L1Cplan), draft, https://oceancolor.gsfc.nasa.gov/data/pace/PACE_L1C_Format_DRAFTv20200918.pdf
11. *The PACE-PAX Validation Traceability Matrix (VTM)*

2 PACE-PAX BACKGROUND

Airborne observations of the land, ocean, and atmosphere by NASA began at the Ames Research Center, which started by acquiring three high altitude U-2 aircraft (designated ER-2 at NASA) and a Convair 990 in 1969 (Bilstein, 1989). Early field campaigns acknowledged the benefit of combining aircraft, land and satellite observations. An example of ground and aircraft validation of satellite observations, the Large Area Crop Inventory Experiment (LACIE), validated crop yield predictions from the Earth Resources Technology Satellite-1, later renamed Landsat-1 (e.g., MacDonald, 1977). Other missions utilized airborne resources to test prototype instruments and measurement techniques, such as described in Sellers et al. (1976) for UV observations of stratospheric ozone, and Hoge and Swift (1981) to map ocean chlorophyll with a lidar. An especially extensive effort was the Global Atmospheric Research Program (GARP, e.g., Perry, 1975) which employed roughly 40 ships, 13 aircraft and 4,000 scientists and technicians for multiple field campaigns. This was a multi-agency, international, effort devoted to harnessing satellite, ground and aircraft observations to improve numerical weather prediction, understanding of climate, and other aspects of the atmosphere. Field campaigns have also been used to support mission formulation, by flying prototype instruments to test observation strategies. Recent examples of this include the Hyperspectral Infrared Imager (HyspIRI) field campaigns (Lee et al., 2015) and the Aerosol Characterization from Polarimeter and Lidar (ACEPOL, Knobelspiesse et al., 2020) field campaign, which was in support of the Aerosol, Cloud, Ecosystems (ACE) mission pre-formulation study (Da Silva et al., 2020). Field campaigns primarily devoted to scientific objectives can also serve the purposes of satellite mission development and validation. Ongoing examples include aerosol-cloud campaigns such as Aerosol Cloud meTeorology Interactions oVer the western ATlantic Experiment (ACTIVATE, Sorooshian et al., 2019) or those focused on a better understanding of ocean biogeochemistry, such as EXport Processes in the Ocean from Remote Sensing (EXPORTS, Siegel et al., 2016, 2021).

The difficulty of gathering validation observations from existing field campaigns was highlighted in the first PACE Science Team, which noted the rarity of observations useful for MAP algorithm development (e.g., https://pace.oceansciences.org/docs/sci2017_proxy.pdf).

A dedicated field campaign is required to support the PACE mission. Experience with pre-launch field missions have demonstrated that validation of new products from PACE requires a targeted effort (PACE-PAX). This is especially the case for the capabilities of MAPs and OCI's UV and hyperspectral sensitivity, from which an extensive set of new geophysical products are derived that are not regularly observed on the ground.

In order to organize of ways in which a dedicated field campaign can be used to validate PACE observations, we have identified a set of observational objectives. The enumerated reasons for conducting a dedicated PACE validation field campaign, in Section 1.1, corresponds to this list, which is based upon successful validation efforts by previous missions. These will be used as a guide to design the PACE dedicated field campaign as well. Starting from these objectives, we will model the flow of a Science Traceability Matrix (STM, e.g., in the PACE SDT report), starting from observational objectives, to the measurement approach needed to satisfy that objective, to the requirements for successful observation and other needs. We will use the analogous name Validation Traceability Matrix (VTM). Once established, the VTM will be used for trade studies while planning the PACE post-launch field campaign. For example, different aircraft, instrumentation, or deployment location scenarios can be compared in the context of their ability to meet observational objectives. This can be accomplished with the use of an adapted Bayesian search theory (BST, Stone, 1989), where estimates of probable success can be assigned to the requirements of each field campaign scenario, and via the VTM, be translated into the probability of meeting an objective. Combined with a decision algorithm, this approach can also be used during a field campaign to guide daily operations (Small et al. 2011). A simplified version of this was used during the ACEPOL field campaign, where a 'scorecard' of measurement objectives informed flight planning.

3 VALIDATION TRACEABILITY MATRIX (VTM)

The VTM is used to connect validation objectives with the design requirements for a successful validation field campaign. The VTM identifies the resources required to conduct a field campaign, and the means to compare different design options. Our implementation makes use of numerical assessments of different components of the VTM, which can be incorporated into planning tools by the use of BST (this aspect is described in more detail in Section 4).

It also can be used to determine the impacts of descoping or loss of elements, and, when combined with BST, a useful tool for mission operations while underway. The categories of information in the VTM are described in the subsequent sections.

3.1 Validation objectives

The objectives are high level goals for the validation, from which all other components of the VTM flow. They were briefly described in the introduction, and more details are provided here.

Objective 1: Validate new retrieval parameters. This is the primary focus of PACE-PAX, addressing the output from algorithms described in the PACE data products table (https://pace.oceansciences.org/data_table.htm) that are not a part of the required products in Tables 2 and 3. We limit our scope to radiometric and polarimetric products, with a focus on observations that can be made from aircraft and those that are complementary to aircraft observations. Many of the products will be produced by algorithms of provisional maturity, validation is necessary to ensure further maturity (see https://science.nasa.gov/earth-science/earth-science-data/data-maturity-levels). An important component of this is the use of airborne proxies of the instruments on PACE. With these proxies, algorithms can be tested in controlled (or at least known) environments, without the need for concurrent PACE measurements. This has been the only feasible approach to validate developing algorithms in the PACE prelaunch era (e.g., Fu et al., 2019, Gao et al., 2020, Puthukkudy et at., 2020), and will remain important after launch.

Furthermore, many algorithms retrieve multiple parameters simultaneously (as described for the MAPs by Dubovik et al., 2014, 2019, Gao et al., 2019, 2020, 2021, Hasekamp et al., 2011, 2019, Puthukkudy et al., 2020, Stamnes et al, 2018) while others require the output of other algorithms as an input (see Frouin et al., 2019 for a description of the use of atmospheric correction for Ocean Color remote sensing). Validation of these algorithms thus requires simultaneous observation of multiple parameters in order to meet this objective.

Aerosol single scattering albedo (SSA) is an example of the type of parameter validated with this objective. Defined as the ratio of scattering to total extinction by aerosols, SSA is not a required product for OCI, but is a climatologically important parameter that can be retrieved from MAPs (Mishchenko et al., 2004, Knobelspiesse et al., 2012, Hasekamp et al., 2019) or inferred from OCI's UV spectral capability (e.g., Torres et al., 2007). Algorithms to determine SSA from PACE measurements are under development by the SAT, project science office, and instrument teams. All these algorithms retrieve multiple parameters and cannot be fully validated as part of the PVP. A specific field effort must therefore be made to validate SSA, and similar products, from PACE.

Objective 2: Assess spatial and temporal scale impact on validation. This is important to link ground, aircraft and satellite observations. Spatiotemporal mismatch between these measurements can be an apparent source of discrepancy unrelated to retrieval accuracy. To complicate matters, this spatial and temporal variability differs among geophysical parameters and conditions (Sayer, 2020, Dickey et al., 2006). We must therefore determine appropriate validation scales, by the use of spatial or temporal surveys. Remote sensing measurements, at a higher spatial (or temporal) resolution than PACE, are best suited for this purpose, as are extended measurements under conditions of known variability.

Objective 3: Validate within the instrument swath of all PACE instruments. While the OCI and HARP2 instruments have a wide swath with 1-to-2-day global coverage, SPEXone has a much narrower (~100km at nadir) swath, resulting in an approximately 30 day global coverage. This means that comparisons of SPEXone to fixed ground locations (such as AERONET) will be infrequent. As an example of the consequences of this narrow swath, we investigated the number of aerosol optical depth (AOD) MODIS-Aqua (e.g., Hsu et al., 2013) to AERONET-OC (Zibordi et al., 2010) validation matchups in the SeaWiFS Bio-optical Archive and Storage System archive (SeaBASS, Fargion et al., 2001) for a three year period (2012-2015) as a surrogate for consequences of instrument swath. In this period, 1,164 and 916 matchups can be found with the subset of MODIS measurements corresponding to OCI and HARP2 swaths, respectively. Restricting to the SPEXone swath results in only 80 matchups in the same time period. Three years is the planned PACE observatory lifetime, which calls into the question the ability to validate narrow swath observations with ground measurements alone. The solution is to position validation assets within the swath of an expected SPEXone observation. This has been a successful approach for other narrow swath instrumentation, such as for the Cloud-Aerosol Lidar and Infrared Pathfinder Satellite Observation instrument (CALIPSO, McGill et al., 2007, Hlavka et al., 2012).

Objective 4: Validate radiometric and polarimetric parameters prior to their use for retrieval of geophysical parameters with instrument proxies (Table 4). This activity supports PACE in-flight calibration activities. For example, during the ACEPOL field campaign (ACEPOL, Knobelspiesse et al., 2020), a team characterized the reflectance of Rosamond Dry Lake in California, providing a bright surface calibration reference. This type of characterization is routinely used to directly validate satellite observations uncertainty models or be used to characterize airborne proxy remote sensing instruments which are subsequently compared to satellite observations.

Objective 5: Target specific geometries, season, and time of day. Retrieval capability depends on observation geometry (the solar and sensor zenith and azimuth angles). This is especially the case for the MAP instruments (e.g., Hasekamp and Landgraf, 2005, Hasekamp et al., 2019, Knobelspiesse and Nag, 2018). Furthermore, a field campaign can be used to investigate the influence that geometry has on retrieval success.

Objective 6: Focus on specific processes or phenomena to verify they are properly accounted for in the satellite retrieval scheme. A variety of atmospheric, ocean, and land surface parameters will be retrieved from PACE observations, and data processing must have the capability to identify when the appropriate algorithms are to be used. Furthermore, those algorithms must be robust for the range of possible conditions that are to be observed. Dedicated field campaigns can seek to observe specific geophysical conditions and ensure retrieval success.

3.2 Measurement objectives

Each top-level objective is further split into measurement objective categories, such as “cloud parameters” or “(cloud-free) aerosols over the ocean”. These categories comprise a set of geophysical parameters retrieved from algorithms that derive them simultaneously, and/or for validation of parameters that have broadly similar mission requirements.

3.3 Measurement objective importance

This is a subjective, numerical measure used to provide a relative weighting of measurement objectives (higher means more important). This weighting is used in assessment of field campaign plans (Section 4), and previous field missions (Section 5) and in support of planning during an ongoing field campaign (Section 8). It should express not only the importance of the measurement objective, but the algorithm maturity for PACE data production of the measurements comprising an objective. The numerical values of this weighting are irrelevant so long as they are consistently applied for all measurement objectives, as it is normalized by the sum of all weights in later analysis.

3.4 Geophysical parameters

These are the individual parameters to be measured or retrieved (Decadal Survey for Earth Observation, NAS 2017), comprising each category of measurement objectives, including parameters of physical, chemical, geological or biological origin. For example, aerosol optical depth (AOD).

3.5 Instruments

These are the instruments capable of observing a geophysical parameter, such as an airborne multi-angle polarimeter. This can either be a direct, remote or proxy validation instrument (described below), and identified as such in the next category. The VTM describes the type of instrument, but not an individual instrument if multiple options exist. Furthermore, the VTM may list several types of instrument options, only one of which is needed unless otherwise noted.

3.6 Instrument type

Direct, *Remote*, and *Proxy* validation refers to different categories of instrumentation. *Direct* instruments measure the targeted geophysical property *in situ*. For example, a Cloud Droplet Probe (CDP, e.g., Faber et al., 2018) measures the liquid cloud droplet size distribution from the wing of an aircraft, and represents that geophysical parameter in that discrete time and place. *Remote* (sensing) instruments may be deployed within the observed scene, but remotely assess geophysical parameters by interpreting how they interact with that scene, such as by scattering sunlight. The geophysical parameter determined from a remote instrument may represent a different physical location than a direct measurement. *Proxy* instruments are a subset of remote sensing instruments, but have characteristics similar to an instrument on PACE, and employ similar algorithms. The AirHARP and SPEX Airborne instruments (McBride et al., 2020, Puthukkudy et al., 2020, Smit et al, 2019a,b) are examples of PACE proxies for the HARP2 and SPEXone instruments, respectively. Table 5 describes and contrasts these types. The choice of which instrument type is most appropriate to satisfy a measurement objective depends on the characteristics of that objective. In most cases it is preferable to have a proxy and either remote or direct instruments available. In situations where this is not possible, proxy measurements may suffice.

Table 5 Instrument measurement types

Instrument type definition	
Proxy	Proxy validation is the use of airborne remote sensing instruments similar to those on PACE, utilizing the same or very similar retrieval algorithms.
Remote	Remotely sensed validation uses retrievals of validation parameters from instruments dissimilar to those on PACE.

Direct	Direct validation is the use of *in situ* sampling of atmospheric, ocean or land parameters.

3.7 Instrument requirements

These are general deployment needs for the instrument, such as aircraft host. In this case, aircraft capabilities are categorized as three broad types, described in Table 6. For instruments not deployed in aircraft, requirements define the ground site needs, research ship capabilities, etc.

Table 6 Aircraft categories

Aircraft categories	
Type A	High altitude, sufficient to overfly aerosols and clouds, e.g., ER-2, WB-57
Type B	Large payload mid-altitude aircraft, e.g., P-3, DC-8. Includes ability to determine if aerosols or clouds are above current flight path, and capability to fly above if needed.
Type C	Small payload low to mid-altitude aircraft, e.g., B-200, Twin Otter

3.8 Mission requirements

These are the physical conditions and other needs for successful validation, such as weather conditions. These fall into a variety of categories, which may or may not be defined based upon the objectives and measurements.

3.8.1 Mission requirements – Surface

The nature of the ocean or land surface in the observed scene.

3.8.2 Mission requirements – Aerosol

Aerosol conditions in the observed scene.

3.8.3 Mission requirements – Cloud

Cloud conditions in the observed scene.

3.8.4 Mission requirements – Other instrumentation

In some cases, measurement requirements require concurrent observation by multiple instruments. For example, if an airborne proxy instrument type is listed in this row, a corresponding ground-based measurement that is desired would be listed here.

3.8.5 Mission requirements – Satellite

If coordinated observations with satellite overflight is desired, those requirements are listed here. This is sometimes the case for direct or remote instrument measurement types.

3.8.6 Mission requirements – Platform

This requirement refers to the circumstances of the instrument hosting platform. For example, and airborne proxy instrument may require observation in a specific solar geometry, or assurance that cirrus clouds are not present above the aircraft.

3.8.7 Mission requirements – Observation time

The length of time required for a 'successful' observation. For airborne field campaigns, this refers to flight hours, including transit time to and from the observation target region, and is deployment region specific. This is a parameter that feeds into a detection probability function (*b(t)*, where *t* refers to time) under the principles of Bayesian optimal search theory (Stone, 1989), which we adapt to the assessment of field campaign plans (Section 4), previous field missions (Section 5) and in support of planning during an ongoing field campaign (Section 8). We will use the exponential detection function

$$b(t) = 1 - e^{-\frac{t}{h}} \tag{1}$$

where h is the observation time. This function describes a case where the probability of successful observation is zero at $t=0$, roughly 63% at $t=h$, and asymptotically approaches 100% as t increases (it is 95% for $3h$). There are other possible detection functions, but in addition to being physically realistic, this has the advantage of a simple derivative, which will be put to use in Section 8.

3.8.8 Mission requirements – Other

Other requirements not previously mentioned.

The draft PACE VTM can be found on the internal cloud instance here: https://nasa.sharepoint.com/teams/PACEscience224/_layouts/15/Doc.aspx?OR=teams&action=edit&sourcedoc={4CABD9AD-4372-42FD-8167-FEC615FB4E17}

Table 7 Validation Traceability Matrix (VTM) summary, where value of *w* (importance of parameter in reaching the validation objective) increases with importance.

Validation objectives	ID	Measured parameters	Importance, w	Objective total
1. Validate new retrieval properties	A	Land surface parameters	2	34
	B	Ocean radiometric parameters	2	
	C	Aerosol parameters over the ocean	10	
	D	Aerosol parameters over land	10	
	E	Cloud parameters	10	
2. Assess spatial and temporal scale impact on validation	F	Cloud parameters	4	6
	G	Aerosol parameters	2	
3. Validate in a narrow swath	H	Aerosol parameters over the ocean	10	20
	I	Aerosol parameters over land	10	

4. Validate radiometric and polarimetric properties	**J**	Validate large reflectances	2	8
	K	Validate large reflectances with high polarization	2	
	L	Validate large reflectances with low polarization	2	
	M	Overfly vicarious calibration sites	2	
5. Target specific geometries, season, and time of day	**N**	Aerosol over ocean retrieval geometry dependence	1	3
	O	Aerosol over land retrieval geometry dependence	1	
	P	Cloud property retrieval geometry dependence	1	
6. Focus on specific processes or phenomena	**Q**	High aerosol loads over land	1	10
	R	High aerosol loads over ocean	1	
	S	Multiple aerosol layers	1	
	T	Aerosol under thin cirrus	1	
	U	Aerosol above liquid phase cloud	1	
	V	Broken clouds with complex structure	1	
	W	Dust aerosols	1	
	X	Aerosol and ocean retrievals over turbid waters	1	
	Y	Aerosol and ocean retrievals over productive waters	1	
	Z	Aerosol and ocean retrievals in and out of glint	1	

4 VALIDATION PLAN EVALUATION

The VTM is a necessarily complex document. But it can be a useful tool for the implementation of a validation field campaign, assessment of prior campaigns, or can inform day to day operation during an ongoing campaign (by guiding flight planning, for example). To do so, we have adapted elements of Bayesian search-and-rescue theory (Stone, 1989). Rather than assessing the likelihood of finding a distressed ship in a grid of geographic locations, we assess the likelihood of meeting a set of measurement objectives.

We have defined several metrics to help assess the relative merits of implementation plans, for which specific instruments and deployment scenarios have been selected. These metrics incorporate the design of the VTM and subjective assessments of the relative importance of those design elements, the capacity of a specific field campaign to satisfy them, and the ability to meet mission requirements.

"Validation instrument potential", V [unitless], expresses the ability of the set of instruments in a given field campaign plan to address measurement objectives, independent of mission length. It incorporates two subjective assessments:

a) the weight assigned to each measurement objective (w, defined as importance in the VTM), and

b) the completeness to which the chosen instrumentation is able to make the required measurements (*c*, unitless and between 0 for no ability and 1 for perfect ability). Some instrument choices may be a less than perfect match to the VTM requirements. For example, a chosen instrument may not have a required spectral channel or may not be deployable in all the required conditions. In such cases, *c* is assigned a subjective assessment value between 0 and 1.

In this manner we can prioritize instruments of varying capability. *V* is thus simply defined:

$$V = \frac{\sum_{i=1}^{n} w_i c_i}{\sum_{i=1}^{n} w_i} \tag{2}$$

where *n* is the number of measurement objectives, and *i* is an index to each. *V* can have values between 0 and 1, where the latter indicates a perfect instrument potential. This metric can be considered instantaneous and does not incorporate deployment considerations such as location and available time.

V is useful to evaluate different instrument configurations, but a full assessment also requires knowledge of the detection probability function, *b(t)*, defined in equation 1, and *p,* the probability of encountering favorable measurement conditions, which incorporates knowledge of weather climatology and other matters pertaining to success.

Our detection probability function is thus updated to

$$b_i^*(t) = 1 - e^{-\frac{tp_i}{h_i}} \tag{3}$$

where the probably of favorable measurement conditions (*p*) has been incorporated for each of the specific measurement objectives (index of i). Furthermore, an overall field campaign assessment needs to include our measurement objective weights (*w*), but relative to the total of all validation plan objective weights (n, indexed by j). To this end, we define a relative weighting, *z*:

$$z_i = \frac{w_i}{\sum_{j=1}^{n} w_j} \tag{4}$$

Finally, we define the time dependent field campaign success, which we call the success function, *S(t)*.

$$S(t) = \sum_{i=1}^{n} c_i\, z_i b_i^*(t) = \sum_{i=1}^{n} c_i \left[\frac{w_i}{\sum_{j=1}^{n} w_j}\right]\left(1 - e^{-\frac{tp_i}{h_i}}\right) \tag{5}$$

This function incorporates our measurement objective weights, *w*, the completeness with which a given instrument configuration meets those objectives, *c*, the amount of time required to make a measurement, *h*, and the probability that favorable conditions exist at a given time during the field campaign, *p.* It is important to note that, with the exponential detection function we have defined, $S(t) = V$ as t approaches infinity (instrument capabilities at maximum measurement time). It is also possible to augment the success function with distribution functions of probability (probably most feasible for *p*), in which case *S* would represent the probability distribution of success as a function of time.

Table 8 Validation assessment metrics for theoretical field campaign Alpha. V=0.78

Measurement objective	Measurement objective weight, *w*	Observation time required, *h*	Measurement completeness, *c*	Probability of success, *p*
A	4	20	1.0	0.5
B	2	10	1.0	0.5
C	2	15	0.0	0.1
D	1	5	1.0	0.1

Table 9 Validation assessment metrics for theoretical field campaign Beta. V=0.75

Measurement objective	Measurement objective weight, *w*	Observation time required, *h*	Measurement completeness, *c*	Probability of success, *p*
A	4	20	0.75	0.75
B	2	10	0.75	0.75
C	2	15	0.75	0.2
D	1	5	0.75	0.2

Table 10 Validation assessment metrics for theoretical field campaign Gamma. V=0.5

Measurement objective	Measurement objective weight, *w*	Observation time required, *h*	Measurement completeness, *c*	Probability of success, *p*
A	4	20	0.25	0.9
B	2	10	0.25	0.9
C	2	15	1.0	0.95
D	1	5	1.0	0.75

To illustrate the value of this function, we compare three field campaign configurations described in Table 8 (field campaign 'Alpha'), **Error! Reference source not found.**9 (field campaign 'Beta'), and **Error! Reference source not found.**10 (field campaign 'Gamma'. All have identical measurement objectives, weights assigned to those objectives (***w***), and requirements on observation time (*h*), but instrumentation used has different capabilities allowing for measurement completeness (*c*). The Alpha field campaign makes complete measurements for three of the four objectives, while the Beta field campaign makes slightly incomplete measurements for all four but has a slightly higher probability of success. Gamma has a clearly deficient capability for the most important objective and for one of the moderately important objectives, but a much higher probability of success.

We choose these configurations to illustrate the interplay between different choices possible in a field campaign. Alpha and Beta have very similar values of validation instrument potential (V), but different success functions, as shown in Figure 1. The steeper initial slope for Gamma (purple) indicates that it may be a viable strategy for field campaigns with shorter available time but is limited in its ability to fully meet mission success. The higher asymptote for Alpha (red) and Beta (green) indicates that they are a better choice with greater time resources. We would also like to note that time, t, is not the same as the flight hours needed for a field campaign, since the success function presumes all measurements are made simultaneously, among other factors. Instead, this function should be used as a mission comparison tool. Section 8 is a more detailed guide for flight planning underway field campaigns.

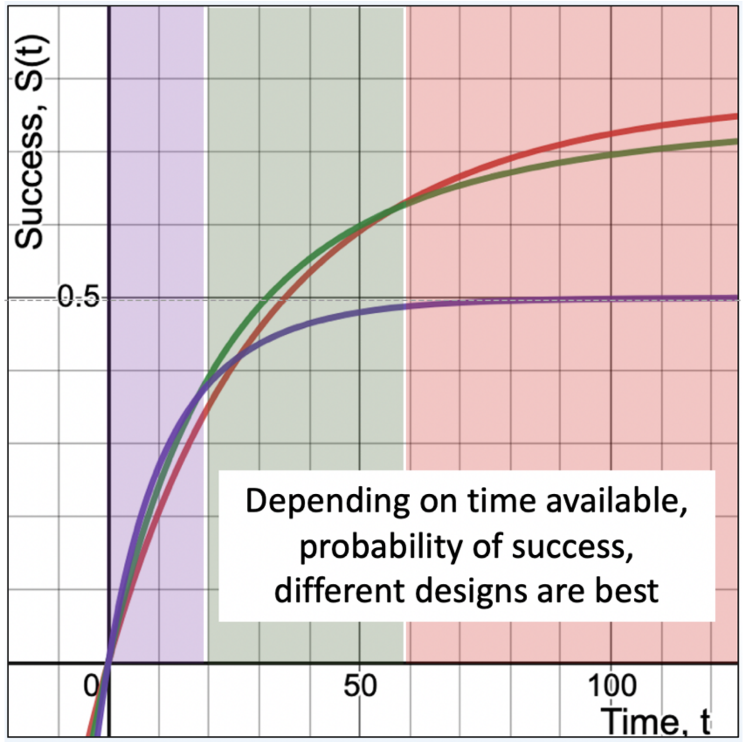

Figure 1 Success functions (equation 5) for field campaign Alpha (red), Beta (green), and Gamma (purple).

These example field campaigns are of course much simpler than our VTM, but they demonstrate how the V and $S(t)$ can be used to aid configuration and deployment choices. As mentioned previously, the metrics are only as good as the subjective assessments that go into them. Their value is in how they reduce the complex, multi-parameter, subjective choices needed for designing a field campaign into combinations of simple assessments.

5 ASSESSMENT OF PREVIOUS FIELD MISSIONS

5.1 Scoring mechanism

We use the validation instrument potential, V (defined in Section 4, equation 2), as a means to assess previous field campaigns in their ability to meet the measurement objectives as described in our VTM. In this case, measurement completeness, c, describes the actual success in making the measurements required for an objective. Deployed instrumentation for a given field campaign are compared to the VTM and scored in terms of this completeness and the weights of the associated measurement objectives, to determine V. In this way, we can understand how the configuration of previous field missions, designed for other purposes, could serve the needs of a PACE validation field campaign.

We use the following scoring to assess previous field missions. Objectives are judged at the measurement objective level. Those for which measurements were made, and data were used for that objective, are assigned a (maximum) score of 1. A score of 0.75 is assigned to objectives for which measurements were made but the data have not yet been assessed. Lower scores are assigned to measurements that are incomplete or had unfavorable conditions (or both).

5.2 ACEPOL

The Aerosol Characterization from Polarimeter and Lidar (ACEPOL) airborne field campaign was conducted from the NASA Armstrong Flight Research Center (AFRC) in Southern California in the fall of 2017 (Knobelspiesse et al., 2020). The high-altitude ER-2 aircraft carried six instruments: four multi-angle polarimeters (AirMSPI, RSP, AirHARP and SPEX Airborne, the latter two of which are airborne proxies of PACE instruments) and two lidars (CPL and HSRL-2). Flights were performed over a variety of conditions, coordinated with ground-based instrumentation (AERONET, AERONET-OC, a ground characterization team at Rosamond Dry Lake, etc.).

ACEPOL was conducted as part of the Aerosol-Cloud-Ecosystems (ACE) mission study (da Silva et al., 2020), and also received funding from the Netherlands Institute for Space Research (SRON) and Cloud-Aerosol Lidar and Infrared Pathfinder Satellite Observations (CALIPSO, Winker et al., 2009) Mission for instrument development and validation. ACEPOL differed from field campaigns with narrow, scientific, objectives: it structured to observe a wide variety of conditions, which were prioritized with the use of a 'scorecard' similar to our VTM.

Our assessment of the Validation Instrument Potential, *V*, for ACEPOL is 0.567.

In many ways, the ACEPOL field campaign contains many of the components of a successful PACE validation field campaign. It deployed two PACE polarimeter proxies and had a complement of two different lidars on board a high-altitude aircraft. It flew in a wide variety of conditions over land and ocean and included coordinated observation with ground sites and satellite overflight. The following were some of the most important missing elements, with potential increases in V had they been included.

1. An appropriate UV-SWIR imager to act as a PACE OCI proxy. Gao et al., (2020) approximated this proxy by combining data from the RSP multi-angle polarimeter (which has SWIR channels) with the SPEX Airborne (which is hyperspectral in the VIS), but UV measurements were not available ($V + 0.018$).
2. More complete ground measurements of Remote Sensing Reflectance. A single AERONET-OC instrument site was available for this purpose ($V + 0.049$).
3. More observations with moderate to high aerosol optical depth. Surprisingly for this part of the world and season, there were few forest fires and minimal air pollution in both the California Central Valley and Los Angeles basin during the period of ACEPOL. To compensate, targets were found farther afield, requiring additional flight hours ($V + 0.080$).
4. More observations with liquid phase clouds, especially marine stratocumulus clouds ($V + 0.167$).

To illustrate the use of V, we also tested the impact of elimination of the lidars onboard the aircraft during ACEPOL. This served to decrease the V by 0.068. However, it is important to note that the impact of this descope (and the enhancements describe above) are affected by other conditions. For example, ACEPOL was not able to observe high aerosol loads over the ocean or multiple aerosol layers. Had those observations been made, the lidar descope would have had a larger impact.

Generally speaking, ACEPOL was a successful field campaign for its purposes, and also served as a resource for PACE pre-launch algorithm development and testing. Examples of research using ACEPOL data for instrument and algorithm development relevant to PACE include Gao et al, 2020, 2021, Hannadige et al, 2021, Fu et al., 2019, Martins et al., 2018, McBride et al, 2020, Puthukkudy et al, 2020, Smit et al., 2019a, b.

6 INSTRUMENT EXAMPLES

The validation objectives described in the VTM are met by deploying a variety of instrument types and configurations. This section provides general background on capabilities and requirements of these instruments but does not necessarily indicate the specific suite of instruments that will be deployed as part of PACE-PAX.

6.1 Dry lakebed surface reflectance characterization

Because of their spatially uniform topography and reflectance, unvegetated dry lakebeds (playas) can serve as a reflectance reference for overflying sensors. Observation with dedicated ground-based characterization in such locations can meet the needs of validation objective #4 in PACE VTM "Validate radiometric and polarimetric properties". Additionally, retrieval of some categories of atmospheric and surface properties can be validated (VTM measurement objectives 1A, 1D, primarily), since surface and atmospheric properties are either retrieved simultaneously, or depend on the validity of assumptions about the other. Several playas exist in the western United States that have been used for this purpose, including Rogers and Rosamond dry lakes in California, and the Railroad Valley Playa in Nevada. To support such activities, ground teams deploy to these locations during overpass, and characterize surface BRDF, atmospheric conditions, and other relevant properties. Examples include activities at Rosamond Dry Lake during ACEPOL (Knobelspiesse et al., 2020) and Railroad Valley Playa during the Fire Influence on Regional to Global Environments and Air Quality (FIREX-AQ) field campaign (Bruegge et al., 2021).

6.2 Sun photometer/sky radiometers

Ground based sun photometers and sky radiometers can provide useful point validation of aerosol (and to a lesser extent, cloud) properties. Sun photometers make a direct measurement of aerosol optical depth (AOD), which defines the optical extinction of the total atmospheric column, by accurately measuring solar radiation through a narrow field of view collimator (Volz, 1959). Many can also act as sky radiometers, from which aerosol optical and microphysical properties can be retrieved (e.g., Dubovik et al., 2000). Zenith measurements in cloudy conditions can also be used to determine the cloud optical depth (COD, Marshak et al., 2004, Chiu et al, 2006, 2010).

The Aerosol Robotic Network (AERONET, Holben et al., 1998) is a federated network of hundreds of automated sun photometer / sky radiometers that use uniform data processing and archival (Giles et al., 2019, Sinyuk et al., 2020). They are the gold standard for validation of satellite aerosol data products and the network is a core component of the PVP for established PACE aerosol products. Despite this success, AERONET does have its limitations. The instruments require a non-moving stable platform, so they are located on land or a very limited number of ocean platforms (an exception, in development, is described in Yin et al., 2019). A subset of AERONET, the Maritime Aerosol Network (MAN, Smirnov et al., 2009), is devoted to ship-based observations using handheld sun photometers. However, those measurements are restricted to AOD and a spectrally derived metric describing the ratio of fine to coarse sized aerosols. They are also constrained by the (limited) frequency of manual deployment on ships compared to continuously sampling robotic instruments that comprise the bulk of AERONET. The Ocean Color component of AERONET (AERONET-OC) is another subset comprised of instruments located on ocean platforms (Zibordi et al., 2009, 2010). AERONET-OC instruments make valuable measurements of normalized water leaving radiance in addition to standard AERONET aerosol measurements. Unfortunately, they are scarce – in the coastal USA there are only 4 of them; one in the Pacific Ocean in Southern California Bight (near Newport Beach, CA), one in the Gulf of Mexico, and three in the mid-Atlantic/New England area (one in the Long Island Sound, one in the Chesapeake Bay and one near Martha's Vineyard). Finally, we should note that the aerosol property retrieval capability of sky radiometers such as those in AERONET depend on aerosol quantity. These retrievals are highly uncertain for small amounts of aerosols (Dubovik et al., 2002), meaning that accurate systematic measurements are representative of a subset of global conditions.

In addition to ground-based sun photometer/radiometers, airborne instruments such as the Spectrometer for Sky-Scanning Sun-Tracking Atmospheric Research (4STAR, Dunagan et al. 2013, Kassianov et al., 2012) can be valuable. In addition to providing focused observations in a desired location and exploring spatial variability, specific aircraft observation patterns (such as vertical spirals) can provide profiles of aerosol properties (e.g., Shinozuka et al, 2007, 2010).

Airborne deployment of instrumentation in PACE-PAX will augment AERONET with focused observations of AOD and aerosol microphysical properties over both land and ocean. When feasible, flight plans will overfly AERONET sites, linking PACE-PAX to (long term) AERONET measurements and characterizing the impact of spatial and temporal scale on satellite data product validation (validation objective 2). Because of the potential for better aerosol microphysical product retrievals with passive multi-angle polarimeters, PACE-PAX will extend validation capability to lower aerosol loads. Finally, targeted measurements within the PACE swath can increase the quantity of validation data points for narrow swath PACE/SPEXone observations.

6.3 Vicarious calibration sites

The PACE OCI instrument will measure the radiance exiting at the TOA, $L_t(\lambda)$ (μW cm^{-2} nm^{-1} sr^{-1}), in the UV-Vis-NIR wavelength range. An atmospheric correction algorithm is required to mathematically 'subtract' the contribution of the atmosphere from this TOA radiance and, thus, derive the water-leaving radiance, $L_w(\lambda)$ (μW cm^{-2} nm^{-1} sr^{-1}) i.e., radiance that is either reflected directly from the ocean surface or that exits through the ocean-air interface via scattering processes (see Frouin et al.(2019) and Ibrahim et al. (2019) for an overview of heritage and alternate atmospheric correction approaches). However, the desired uncertainties on $L_w(\lambda)$ retrieval cannot be achieved through instrument pre-launch calibration and characterization alone and must additionally rely upon on-orbit calibration. This process takes the form of a system level calibration, known as system vicarious calibration (SVC). The system referred to in this case is

OCI instrument and processing algorithm which takes $L_t(\lambda)$ as input and removes the atmospheric signal to produce $L_w(\lambda)$ as output. The vicarious calibration process is effectively an inversion of the forward processing algorithm, wherein a known water-leaving radiance, $L_w^t(\lambda)$, is the input and predicted TOA radiance, $L_t^t(\lambda)$, is the output, and where the superscript *t* indicates targeted or predicted values. The ratio of predicted to observed $L_t(\lambda)$ is the vicarious gain: the correction factor that, when applied to $Lt(\lambda)$, would force the system to yield $L_w^t(\lambda)$. A full description of the SVC process can be found in Franz et al. (2007).

SVC makes use of specific calibration sites where instrumentation has been placed for this purpose (often on buoys). These sites may also serve a role in PACE-PAX, in that they can serve as a validation of the ability to retrieve ocean radiometric parameters (validation objective 1B) or the joint retrieval of those parameters alongside aerosol parameters (validation objectives 1C). They can also be used in the SVC context for proxy instruments themselves (validation objective 4M).

The primary SVC site for all NASA ocean color satellites since 1997 (Barnes et al., 2001, Eplee et al., 2001, Franz et al., 2007) has been the Marine Optical Buoy (MOBY, Clark et al. (1997; 2003)). It is a moored buoy located approximately 20 km west of the island of Lanai in 1200 m of water with both an above and below water expression. Above the water, the main components comprise an irradiance, $E_s(\lambda)$ (μW cm^{-2} nm^{-1}), sensor, a GPS unit, a weather station, and communications components. Below the water lies an optical chain with sensor arms at 1, 5, and 9 m that measure downwelling irradiance, $E_d(\lambda)$ (μW cm^{-2} nm^{-1}), and upwelling radiance, $L_u(\lambda)$ (μW cm^{-2} nm^{-1} sr^{-1}). Since measurements are acquired at multiple depths, attenuation coefficients for L_u and E_d can be calculated, k_{Lu} and k_d respectively (m^{-1}), and used to propagate L_u and E_d to just beneath the water surface. These values are then used to calculate water leaving radiance, $L_w(\lambda)$ (μW cm^{-2} nm^{-1} sr^{-1}), which is ultimately utilized in the calculation of gain factors to vicariously calibrate on orbit satellite ocean color sensors.

In addition to MOBY, two SVC teams, which take distinctly different approaches to data acquisition methodology, were selected for a 2019 NASA funding opportunity. The first of these is the Marine Optical Network (MarONet) platform. This is essentially an upgraded version of the MOBY platform and follows the same moored buoy design with sensors located at the surface and three fixed depths. One important difference lies in the fact that updated optics and hardware allow simultaneous acquisition of $E_s(\lambda)$, $E_d(\lambda)$, and $L_u(\lambda)$. MOBY acquires each of its $L_u(\lambda)$ measurements separated by several minutes that can, potentially, result in uncertainty when combining measurements to derive parameters such as a vertical attenuation coefficient. It is intended that MarONet be deployed near the MOBY site near Lanai, and pending logistical challenges, in waters off of Western Australia. Both sites have been shown to have conditions conducive to the acquisition of high-quality SVC radiometric data (Zibordi and Mélin, 2017). By deploying this system in the same area as MOBY, continuity of measurement is ensured, and new measurements can be compared with the already extensive climatology that exists at this site.

The second of these SVC platforms is the HyperNav system, a Lagrangian, profiling float which can adjust its buoyancy to operate both in a near-surface or profiling mode. The HyperNav measures hyperspectral $L_u(\lambda)$ and $E_d(\lambda)$ but is not equipped with an above water $E_s(\lambda)$ sensor. An integral part of the HyperNav measurement strategy is deployment in known physical oceanographic features intended to retain the float in the same general area for an extended period of time, e.g., ocean eddies. The float's trajectory is predicted by the physical model, which helps to ensure that appropriate conditions for SVC are encountered and improves the chances of successfully retrieving the float at the end of a deployment period. HyperNav has already been deployed near the MOBY site, and future deployments will include the waters surrounding Puerto Rico. HyperNav was intended to be a fully portable system that will allow assessment of various geographical locations for SVC in contrast to the fixed location strategy of the MarONet buoy.

6.4 Wind buoys

Retrieval of aerosol properties over the ocean requires consideration of light interactions both within the ocean body and at the ocean-air interface. The latter can be the source of specular reflection of the direct solar beam, referred to as sun glint or glitter. Depending on sun – observation geometry, ocean surface roughness and other factors, glint can be significant enough that it must be considered in the retrieval process. In some cases, it is so large that it dominates the total signal and preclude the retrieval of other properties. The magnitude and direction of glint is driven by ocean surface roughness, the statistical distribution of the surface slopes. This roughness is linked to, and often parameterized by, surface winds (Cox and Munk, 1954). Knowledge of surface wind speed and direction is therefore important for the remote sensing of the atmosphere and ocean at geometries potentially affected by glint. In algorithms for single view angle instruments, wind speed is required as an input to either avoid or account for glint (e.g., Wang et al., 2001), whereas multi-angle instruments such as HARP2 and SPEXone have the ability to simultaneously retrieve aerosol, ocean and wind properties (e.g. Fox et al., 2007, Fu et al., 2019, Gao et al., 2021, Knobelspiesse et al., 2021, Stamnes et al., 2018).

Thus, validation of aerosol and ocean retrieval algorithms require information on surface wind vector. Fortunately, the National Oceanographic and Atmospheric Administration (NOAA) maintains an extensive network of wind speed monitoring buoys, the National Data Buoy Center (NDBC, https://www.ndbc.noaa.gov/). This network of instruments are well located, often in the immediate vicinity of AERONET-OC sites. Successful PACE-PAX flight plans will require overflights of these buoys.

6.5 Direct sampling of aerosols and clouds

Measurements of cloud and aerosol properties can be made by sampling from an aircraft flying through a cloud or aerosol plume. Airborne 'Direct' measurements are identified in many parts of the VTM (see Section 3.6), and they are also necessary to for comparison to 'Proxy' measurements when there is no satellite overflight or ground based Direct measurements to compare to.

Direct measurements represent a point in time and space, and as such care must be taken when comparing to satellite or airborne remote sensing observations which represent a larger spatial extent, the entire atmospheric column, and other differences. From an airborne field campaign planning perspective, the deployment of both Direct and Remote or Proxy instruments also presents a challenge, as the Direct measurement is made within the cloud or aerosol plume, while the Remote or Proxy measurements are made from above. A solution is to alternate between Direct and Remote/Proxy with specific maneuvers. An example of this approach was the 2017 and 2018 deployments of the P-3 aircraft during the ObseRvations of Aerosols above CLouds and their intEractionS (ORACLES) field campaign (Redemann et al., 2021, see figure 12 for aircraft maneuvers). While this provides for the means to sample with all three categories of instruments, there are potential drawbacks. One is that making measurements of one type of instrument means that the other types cannot collect meaningful data at the same time. Thus, it takes more flight hours to accomplish objectives, and flight hours must be spent moving from one observation mode to another. There is also time lag between making a Remote/Proxy measurement at high altitude and a Direct measurement within the aerosol or cloud. The geophysical state may change during that interval, and careful management of the aircraft flight plan is needed to ensure that the Direct and Remote/Proxy measurements are comparable. The advantage of this approach is that all measurement types can be made with a single aircraft.

Alternatively, Direct and Remote/Proxy observations can be made simultaneously with separate platforms. While the use of multiple aircraft can mean higher costs, the selected aircraft can be well suited for their respective roles and use flight hours more efficiently. The Imaging Polarimetric Assessment and Characterization of Tropospheric Particulate Matter (ImPACT-PM, Kalashnikova et al., 2018) is an example of this approach that may be a (smaller scale) model for PACE-PAX. The purpose of that campaign was to validate AirMSPI retrieval capability of smoke aerosol properties in preparation for the launch of the Multi-Angle Imager for Aerosols (MAIA, Diner et al., 2018) instrument. AirMSPI, serving as a proxy for the MAIA instrument, was deployed on the high-altitude ER-2 aircraft (see Section 7.2) from ARFC. It overflew the US Naval Postgraduate School's Center for Interdisciplinary Remotely Piloted Aircraft Studies (CIRPAS) Twin Otter, outfitted with aerosol and cloud direct sampling instrumentation. The CIRPAS Twin Otter, deployed from Marina, CA, made coordinated observations with the ER-2 of smoke plumes in central California.

The CIRPAS Twin Otter aircraft can be fitted with a variety of instruments that measure aerosol and cloud properties. As summarized in Table 11 CIRPAS Twin Otter instruments. This table contains facility instruments only, others can also be added.Table 11, these instruments include:

- Those that measure navigation (position, attitude, altitude, airspeed, etc.), meteorology (temperature, pressure, dew point, etc.) and wind speed and direction.
- CN/Ultrafine: cloud condensation nuclei counter
- Passive Cavity Aerosol Spectrometer Probe (PCASP): binned aerosol particle concentration from 0.1 to 3.0μm.
- Cloud Aerosol and Precipitation Spectrometer (CAPS): multiple instrument suite, for measurements of cloud droplet and aerosol concentration from 0.5 to 50μm (Cloud and Aerosol Spectrometer, CAS), concentration of cloud particles from 50 to 1600μm (Cloud Imaging Probe, CIP), and liquid water content (Hotwire LWC).
- Forward Scattering Spectrometer Probe (FSSP): optical probe for determination of cloud particle size (similar to the CAS).
- Scattering Nephelometer: measures the aerosol dry scattering coefficient in at three visible (VIS) wavelengths.
- Particle Soot Absorption Photometer (PSAP): determines aerosol absorption at three VIS wavelengths.
- Broadband / Infrared solar radiation: determines light field for radiative closure studies and other purposes.

Table 11 CIRPAS Twin Otter instruments. This table contains facility instruments only, others can also be added.

Instrument	Observed geophysical parameters	Validation Objective
Navigation	Position, attitude, airspeed, etc.	n/a
Meteorology	Temperature, pressure, dew point	n/a
Wind	Wind speed and direction, vertical winds	n/a
CN/Ultrafine	Aerosol cloud condensation nuclei	n/a
PCASP	Aerosol fine mode size distribution	1c, 1d, 2g, 3h, 3i, 5n, 5o, 6q, 6r, 6s, 6t, 6u, 6w, 6x, 6y, 6z
CAPS	Instrument suite for aerosol and cloud counts and size distributions, plus liquid water content	1c, 1d, 1e, 2f, 2g, 3h, 3i, 5n, 5o, 5p, 6q, 6r, 6s, 6t, 6u, 6v, 6w, 6x, 6y, 6z
FSSP	Optical cloud and aerosol particle sizing	1e, 2f, 5p, 6t, 6v
Scattering Nephelometer	Dry aerosol scattering at three VIS wavelengths	1c, 1d, 2g, 3h, 3i, 5n, 5o, 6q, 6r, 6s, 6t, 6u, 6w, 6x, 6y, 6z
PSAP	Aerosol absorption at three VIS wavelengths	1c, 1d, 2g, 3h, 3i, 5n, 5o, 6q, 6r, 6s, 6t, 6u, 6w, 6x, 6y, 6z
Broadband Solar Radiation	Broadband solar radiation	n/a
Broadband IR Radiation	Infrared (IR) solar radiation	n/a

Most of the facility instruments on the CIRPAS Twin Otter can make measurements that trace to objectives in the PACE-PAX VTM, so that aircraft may make a successful platform for Direct measurements to fly in coordination with another aircraft flying Remote/Proxy instruments. Other possibilities include the use of instrument groups such as the NASA Langley Aerosol Group Experiment (LARGE, e.g., Schafer et al., 2019) or notional plans such as the Systematic Aircraft Measurements to Characterize Aerosol Air Masses (SAM-CAAM, Kahn et al., 2017) as a starting point for designing a Direct measurement suite.

6.6 Lidar instruments

Lidar instruments devoted to cloud, aerosol and ocean remote sensing are an ideal complement to the passive observations that will be made by PACE (e.g., Jamet et al., 2019). This is in part because, as active instruments, they interact differently with the geophysical state and can provide information (such as atmospheric and oceanic vertical profiles) to which passive systems are less sensitive (albeit in a narrow swath). For this reason, they can collect useful validation data as part of PACE-PAX, an approach that has been taken in previous airborne field experiments that tested passive instrument remote sensing techniques (e.g., Da Silva et al., 2020, Fu et al., 2020, Gao et al., 2020, 2021, Knobelspiesse et al., 2011a, 2020, Puthukkudy et al., 2020, Xu et al., 2021). Lidar products can be used to validate the advanced aerosol parameters for validation objective 1 (Sec 3.1), make continuous along-track measurements at nadir viewing direction for validation objective 2, and meet the narrow swath requirement for the validation objective 3.

Although lidar systems and capabilities vary (see Ansmann et al., 2013 for a review), we will consider two broad categories of lidar instruments. Backscatter lidars, such as the Cloud Physics Lidar (CPL, McGill et al., 2002, 2007) provide vertical profiles of backscatter and depolarization for clouds and aerosols at discrete UV, VIS and NIR channels. Further analysis can calculate particulate extinction coefficients (which can be vertically integrated to calculate cloud or aerosol optical depth), identify aerosol or cloud layer top and base altitudes, and classify by aerosol type

(Yorks et al., 2011). CPL has been specifically deployed to validate observations from the CALIPSO orbital backscatter lidar (Hlavka et al., 2012), and was one of the instruments on the ACEPOL field campaign (Knobelspiesse et al., 2020), alongside other lidar and multi-angle polarimeter instruments.

Another option is a High Spectral Resolution Lidar (HSRL, Shipley et al., 1983), which, unlike a backscattering lidar, independently observes molecular and particulate return. This provides for a quantitative measurement of particulate extinction without assuming optical properties of the atmosphere, although with additional complexity and cost. The NASA Langley Research Center (LaRC) HSRL-2 has eponymous channels at 355 and 532nm, as well as a backscatter only channel at 1064nm and depolarization ratio sensitivity for all three channels (Müller et al., 2014, Burton et al., 2018). HSRL-2 is a successor of the HSRL-1 instrument (Hair et al., 2008, Rogers et al., 2009, Burton et al., 2012) and has operated since 2012. Retrievals based on HSRL-2 measurements provide standard products such as aerosol optical depth (AOD) and lidar ratio at 355 and 532 nm, as well as derived products such as aerosol mixed-layer heights (Scarino et al., 2014), aerosol type classification (Burton et al., 2012), and aerosol effective radius and concentrations (Müller et al., 2014, Sawamura et al., 2017). Like CPL, the HSRL-2 was deployed on the ACEPOL field campaign.

Table 12 summarizes CPL and HSRL-2 capabilities. β indicates sensitivity to backscatter coefficient, while α denotes extinction coefficient and δ depolarization ration sensitivity.

Instrument	355nm	532nm	1064nm	Data
CPL	β	β	$\beta\delta$	https://cpl.gsfc.nasa.gov
HSRL-2	$\beta\alpha\delta$	$\beta\alpha\delta$	$\beta\delta$	Available with field campaign archives

6.7 Airborne UV-SWIR spectrometers

Identifying a UV-SWIR spectrometer that can act as a proxy for the OCI instrument is a challenging task: it must match the UV-NIR hyperspectral capability and discrete SWIR channels while maintaining a high signal-to-noise (SNR) ratio appropriate for observations of a relatively dark ocean (see Table 1). For background, we describe several potential OCI proxies in detail, acknowledging that there are other potential proxy instruments available as well.

The Airborne Visible / Infrared Imaging Spectrometer – Next Generation (AVIRIS-NG, Chapman et al., 2019) is an instrument with heritage with the venerable Airborne Visible / Infrared Imaging Spectrometer (AVIRIS, Vane et al., 1993), now denoted 'classic'. AVIRIS-NG is a UV-SWIR (380-2510nm) spectrometer with 5nm spectral resolution and a 36˚ field of view, frequently used for studies of surface reflectance (e.g., Thompson et al., 2019, 2020) and trace gases (e.g. Thorpe et al. 2017). Spectrally, AVIRIS covers the range of OCI (except in the lowest wavelengths in the UV), but it has been rarely used for aerosol or ocean remote sensing.

The Enhanced MODIS Airborne Simulator (eMAS, Ellis et al., 2011) is an airborne spectrometer intended to mimic (and exceed) the capabilities of the orbital Moderate Resolution Imaging Spectroradiometer. It has 38 discrete channels, nine in the VIS-NIR (465 to 947nm), the remainder in the SWIR-IR (1.619 to 13.957μm). While these capabilities do not match the spectrometer characteristics of OCI in the UV-NIR, they exceed OCI capabilities in the SWIR-IR, providing for a means to test the capability of products that specifically rely on those channels (clouds). It builds on the heritage of the earlier MODIS Airborne Simulator (MAS, King et al., 1996). Both instruments are operated by the NASA Ames Research Center (ARC).

The Portable Remote Imaging Spectrometer (PRISM) is an airborne spectrometer specifically designed for coastal ocean remote sensing (Mouroulis et al, 2014). It shares many capabilities with the OCI instrument, although with fewer SWIR channels. Like AVIRIS and AVIRIS-NG, it is operated by JPL.

There are, of course, many other airborne spectrometers in use and a full consideration must encompass characteristics in addition to availability and reliability. Characteristics of these three instruments compared to OCI are shown in Table 13.

Table 13 Airborne spectrometer characteristics compared to OCI. Note that the airborne instrument swath width and ground pixel size varies with aircraft altitude, values provided here correspond to an assumed 20km altitude of the ER-2 aircraft.

	OCI	AVIRIS-NG	eMAS	PRISM
UV-NIR range	Continuous from 340 to 890nm in 5-nm steps	Continuous from 380 to 2510 in 5-nm steps	Nine discrete bands from 465 to 947nm	Continuous from 350 to 1053.5nm at 3.5nm resolution
SWIR-IR range	0.940, 1.038, 1.250, 1.378, 1.615, 2.130 and 2.260 µm		29 discrete bands from 1.619 to 13.957µm	Two channels, centered at 1.242 and 1.608µm
Swath width	±56.6˚ (2,663 km at 20˚ tilt)	±36˚, ~26km	37.25km	±36˚, ~11km
Ground pixel	1 km at nadir	600 cross track pixels, ~10m at nadir	50m at nadir	608 cross track pixels, ~18m at nadir (UV-NIR)
Institution	GSFC	JPL	ARC	JPL
Data	At launch	https://avirisng.jpl.nasa.gov/	https://mas.arc.nasa.gov/	https://prism.jpl.nasa.gov/

6.8 Airborne SPEXone and HARP2 proxies

AirHARP and SPEX Airborne instruments (characteristics in Table 14) are the airborne version of the PACE HARP2 and SPEXone, respectively, and therefore ideal validation proxies. AirHARP measures the same spectral and polarization bands with HARP2 (Martins et al., 2018, McBride et al., 2020, Puthukkudy et al., 2020). The difference is that AirHARP measures more viewing angles than HARP2 (a total of 120 vs 90 angles). Meanwhile, SPEX Airborne (Smit et al, 2019a,b) measures a similar spectral range and resolution as SPEX2, but with more viewing angles than SPEXone (nine vs five angles).

Both AirHARP and SPEX Airborne instruments had been deployed in the ACEPOL field campaign and successfully collected scientific data (Knobelspiesse et al 2020). Multi-parameter retrieval algorithms have been developed and applied to obtain aerosol properties (Gu et al 2020, Puthukkudy et al., 2020, Gao et al 2020, 2021) and ocean color signals (Gao et al 2021). Prior to the launch of PACE, these data are valuable for algorithm development and testing. Deployed post-launch as part of PACE-PAX, they would serve as remote and proxy measurements that are at the core of many measurement objectives (see VTM for more details).

Table 14 Instrument specifications for AirHARP and SPEX Airborne. Compare to PACE HARP2 and SPEXone in Table 1.

	AirHARP	SPEX Airborne
Spectral bands (bandwidth)	440 (16), 550 (12), 670 (18), 870 (39) nm	Continuous from 400 to 800 nm in 2-3nm steps
Polarized bands	All	Continuous from 400 to 800 nm in 10-40nm steps
Cross track swath	94˚	7˚
Number of along track viewing angles	20 for 440, 550 and 870 nm and 60 for 670 nm (spaced over 114˚)	9 (0°, ±14°, ±28°, ±42°, ±56°)
Institution	University of Maryland, Baltimore County (UMBC)	Netherlands Institute for Space Research (SRON)

6.9 Airborne multi-angle polarimeters

Besides the AirHARP and SPEX airborne instruments, other MAP instruments with complementary measurement capabilities can add value to PACE-PAX as remote sensing instruments. These include the Research Scanning Polarimeter (RSP), which makes highly accurate polarimetric measurements with a hyper-angular resolution (Cairns et al 1999). Although it is not an imager and has a single pixel swath, it provides high quality aerosol and cloud retrieval products (e.g., Alexandrov et al., 2018, Chowdhary et al, 2002, 2012, Knobelspiesse et all, 2011a, b, Ottaviani et al., 2018, Waquet et al., 2009), and therefore useful to evaluate the retrieval performance from MAP measurements. Moreover, the four RSP SWIR (shortwave infrared) bands provide extra value as important proxies for the OCI SWIR measurements. Another MAP is the Airborne Multiangle SpectroPolarimetric Imager (AirMSPI) which has high spatial resolution and acquires multi-angle observations through the use of a gimbal system. This system has eight spectral channels, three of which have sensitivity to polarization (Diner et al 2013a). AirMSPI has also been used successfully for the retrieval of microphysical properties of aerosols, and to a lesser extent clouds (e.g., Diner et al., 2013b, Kalashnikova et al., 2018, Xu et al., 2018, 2019)

Table 15 Instrument specifications for RSP and AirMSPI.

	RSP	AirMSPI
UV-NIR range (bandwidth)	410 (30), 470 (20), 550 (20), 670 (20), 865 (20)nm	355 (29), 380 (33), 445 (38), 470 (39), 555 (29), 660 (39), 865 (38), 935 (50)nm
SWIR range (bandwidth)	960 (20), 11590 (60), 1880 (90), 2250 (120)nm	None
Polarized bands	all	470, 660, 865

Number of viewing angles	152 (continuous within ± 60˚ in 0.8˚ steps)	Selectable, typically 5 to 9 (± 67˚)
Institution	NASA Goddard Institute for Space Studies (GISS)	Jet Propulsion Laboratory (JPL)

7 MISSION REQUIREMENTS

7.1 Management approach

The PACE-PAX mission will require a dedicated team for successful planning and implementation. Overall, PACE Project Science will lead the mission in collaboration with the PACE Program Scientists at NASA HQ and will select one of its members to lead as the Mission Scientist (MS), described below. Once the planning stage of PACE-PAX has begun, regularly scheduled meetings will occur among the leadership team, with NASA HQ, and among the entire PACE-PAX team (in descending order of frequency).

The PACE-PAX team will include the following members.

PACE-PAX mission scientist (MS): will have an overall responsibility for the field campaign, will lead the PACE-PAX team, and will be the interface between the team and PACE Project Science, NASA HQ, the PACE Validation Science Team (to be competed at a later date), and others. They will be responsible for defining and meeting the validation objectives, their scope, and implementation.

PACE-PAX deputy mission scientist (DMS): will assist the PACE-PAX mission scientist and serve in their place when the MS is unavailable for meetings or other activities.

PACE-PAX project manager (PM): will provide guidance on management aspects to the MS. They will work with the aircraft managers, instrument scientists and other members of the team regarding shipping, deployment of personnel, and other matters pertaining to logistics. They will set the set and maintain the budget and schedule, and work with the Aircraft Manager(s) to ensure risk management and safety.

PACE-PAX instrument scientists (IS): are responsible for integration, deployment and operations for individual scientific instruments.

PACE-PAX Aircraft Manager(s) (AM): Will serve as the point of contact between the PACE-PAX team and the aircraft personnel, including responsibility for instrument integration, planning and operations.

PACE-PAX weather forecasting team (WF): will provide forecasts or climatologies of weather and geophysical parameters during planning and operations of PACE-PAX. Both will be connected to the previously described decision algorithms and BST.

PACE-PAX data manager (DM): will ensure that data collected during the campaign will be archived in accordance with NASA policies in the identified repository.

7.2 Airborne platforms

A majority of the instruments described in the VTM are deployed on an airborne platform. NASA owns and operates a variety of aircraft that can be used for earth science, some of which are managed by the Airborne Science Program (ASP, https://airbornescience.nasa.gov). These aircraft are described in Table 16, with categorical descriptions in Table 6. Aircraft from other government agencies and institutions (NOAA, DoD, NSF) may also be available.

Aircraft categories denote the role that an aircraft may play in a PACE-relevant field campaign. *Category A* aircraft are capable of long-range, high-altitude flights, appropriate for remote and proxy measurements. They must be able to overly most of the atmospheric aerosol column and potential clouds. Often, these aircraft have limited personnel space (e.g., ER-2 and WB-57), so individual instrument scientists cannot fly with the aircraft, so instruments must be autonomous or nearly so. *Category B* aircraft are capable of remote sensing, proxy and direct observations, and generally have larger payloads that support instrument operators. Since these aircraft typically fly at lower altitudes than *Category A* aircraft, successful remote and proxy measurements require the means to check that there are no aerosols or clouds above the aircraft, which upwards looking sun photometers or lidars can provide. These aircraft may not have the capability to overfly high altitude thin cirrus clouds. Direct measurements require the ability to fly within an aerosol plume or a cloud, often with complicated flight patterns. Typically, such maneuvers are preceded or followed by high altitude measurements for remote sensing and proxy measurements. Finally, *Category C* aircraft are smaller and cheaper, but probably not capable of remote or proxy observations due to their lower maximum altitude. These are primarily appropriate for direct observations.

The diversity of aircraft type means that costs are variable, additionally, costing structure varies among the organizations that operate the aircraft. Additionally, deployment location may affect cost. Operating out of an aircraft's home center may minimize ground and aircraft crew travel costs but restricts the study area and may have other consequences (for example, weekend flights may require special approval). Finally, instrument integration costs can be considerable, but lessened if an instrument has been previously integrated on an aircraft. All of these issues mean that trade studies on aircraft selection, configuration and deployment location will be the largest drivers of mission cost.

Table 16 potentially available NASA Aircraft. ASP indicates if the aircraft is managed by the NASA Headquarters Airborne Science Program. NASA Centers are the Armstrong Flight Research Center (AFRC) in Palmdale, CA, the Johnson Space Center (JSC) in Houston, TX, the Langley Research Center (LaRC) in Hampton, VA, the Wallops Flight Facility in Wallops Island, VA, the Ames Research Center (ARC) in Moffett Field, CA, and the Glenn Research Center in Cleveland, OH. Navy refers to the Naval Postgraduate School. * Denotes Unmanned Aircraft System (UAS).

Aircraft	ASP	Center	Category	Range (nm)	Max Altitude (ft)	Endurance (hours)	Payload (lbs.)
B-200	No	LaRC	C	1,200	30,000	6	1,200
C-23 Sherpa	No	WFF	B/C	860	19,000	5	
CIRPAS Twin Otter	No	Navy	C	300	18,000	5	1,500

Cessna 206H	No	LaRC	C	700	18,000	6	800
DC-8	Yes	AFRC	B	5,500	40,000	12	22,000
ER-2 (2)	Yes	AFRC	A	5,000	70,000	12	5,000
Global Hawk*	No	AFRC	A				
Gulfstream C-20A	Yes	AFRC	A/B	3,300	45,000	7	3,400
Gulfstream GIII	Yes	JSC	A/B	3,300	45,000	7	3,400
Gulfstream GIII	Yes	LaRC	A/B	3,300	45,000	7	3,400
Gulfstream GV	Yes	JSC	A/B	5,700	50,000	13	7,500
HU-25C Guardian	No	LaRC	B	2,000	42,000	5	2,500
P-3 Orion	Yes	WFF	B	3,800	30,000	13	14,000
SIERRA*	No	ARC	C	600	10,000	10	
S-3B Viking	No	GRC	B/C		40,000		
Twin Otter	No	GRC	C	300	18,000	5	1,500
WB-57	No	JSC	A	2,400	65,000	7	9,000

7.3 Operations base

Selection of the field campaign operations base (OB) is an important aspect of mission planning. This selection must consider:

1. The OB must have an airport and nearby facilities that can support the selected airborne platform(s). This includes factors such as runway length, availability of logistical support, maintenance facilities, availability and cost of hangar, laboratory and office space, and other factors.
2. The OB must be logistically feasible and minimize costs of deployment to that location for the aircraft, crew, instrument teams and other personnel.
3. The OB must be within aircraft range of the geophysical conditions appropriate to satisfy the VTM objectives. If they are variable (such as the presence of aerosols or clouds) the probability and seasonality of encountering optimal conditions must be assessed.

The NASA centers mentioned in Table 16, all of which have runways, are attractive because they can be a relatively inexpensive OB that satisfies the first and second consideration above. Nearly all of them are in coastal regions (the exception being GRC, which is close to Lake Erie), meaning that they can access both land and ocean sites without wasting flight hours in transit. Additional ease and cost savings can be realized by selecting an OB that is the same as the aircraft's home center. In these situations, the aircraft support crew may not need to incur travel expenses.

If a NASA center with a runway is not selected as an OB, cost savings may be realized by using military aviation facilities (when available), or by locations that have been previously utilized for NASA airborne field campaigns.

Multiple OB locations can also be considered as a means to extend the range of accessible observation locations. This can be achieved by moving the OB location partway through a field campaign, or by performing a 'suitcase flight', by which the aircraft lands in another location than the OB and makes a later return flight. If more than one aircraft is used, different OB's can be used for each aircraft if they are sufficiently close that coordinated flights can be performed together.

Finally, selection of the OB should assess the adjacency of stationary ground measurements, and the restrictions that Special Use Airspace (SUA) can impose on potential flight plans.

7.4 Ground resources

Careful aircraft coordination with ground observation sites (see Sections 6.2 and 6.3) will be an important aspect of PACE-PAX. Overflights should be made when ground measurements are being made, and in a manner conducive to measurement by the airborne instruments. For example, multi- angle polarimeters (see Section 6.9) require long, straight flight segments so that all angles fore and aft observe a target. In many cases these instruments operate best if the flight track is aligned with the solar azimuth angle, so that the widest range of scattering angles are observed.

Figure 2 ACEPOL flight track emphasizing coordination with ground observations. AERONET and AERONET-OC sites are indicated in white, Rosamond Dry Lake with a yellow arrow. The flight track is indicated in green, and the flight began and ended near AFRT just south of Rosamond Dry Lake.

Figure 2 shows an example of close aircraft – ground coordination during the ACEPOL flight on October 25, 2017. On this day, a team from JPL was deployed to Rosamond Dry Lake to characterize surface reflectance (see Section 6.1), and a 'Rosette' of five overflights at various headings were performed. Additionally, the Fresno, Bakersfield, UCSB, USC_SEAPRISM, and CalTech AERONET sites were overflown. The Bakersfield overflight was planned to be within 10˚ of the solar azimuth angle.

7.5 Ocean surface resources

Although PACE-PAX is not directly planning for the deployment of ship-borne instrumentation, it is important to prepare for coordination with ongoing efforts to observe the ocean radiometric state and augment continuous observations by, for example, AERONET-OC sites. Ship borne, direct radiometric measurements can satisfy validation objective 1b, and contribute to validation objectives 1c, 2g, 5n, 6r, 6x, 6y and 6z. Coordinated measurements can be performed in a similar manner as with ground measurements described in the previous section but require close cooperation between the PACE-PAX and ocean observing teams. The role of the DMS will be to seek out potential planned observations at the time of PACE-PAX and within range, connect with those teams, and provide coordination during the field campaign.

7.6 Satellite coordination

Coordinated under-flights of PACE is the primary requirement of validation objective 3, "Validate in a narrow swath" and for validation with measurements that are classified as 'direct' or 'remote' in Section 3.6 (unless those measurements are in support of a 'proxy' measurement). Predictions of satellite flight path will be obtained by the PACE-PAX DMS and incorporated with weather forecasts for the purposes of flight planning. Flight plans satisfying this requirement for instruments in ascending polar orbit like PACE have long, roughly South to North paths, at time of overpass. For example, the ACEPOL field campaign made three CALIPSO or Cloud-Aerosol Transport System (CATS, McGill et al., 2015, Yorks et al., 2016) under-flights. Considering the high importance of objective 3, we expect to make a larger fraction of observations in this mode. Figure 3 is an example of a flight during the ACEPOL field campaign that performed an under-flight of CALIPSO.

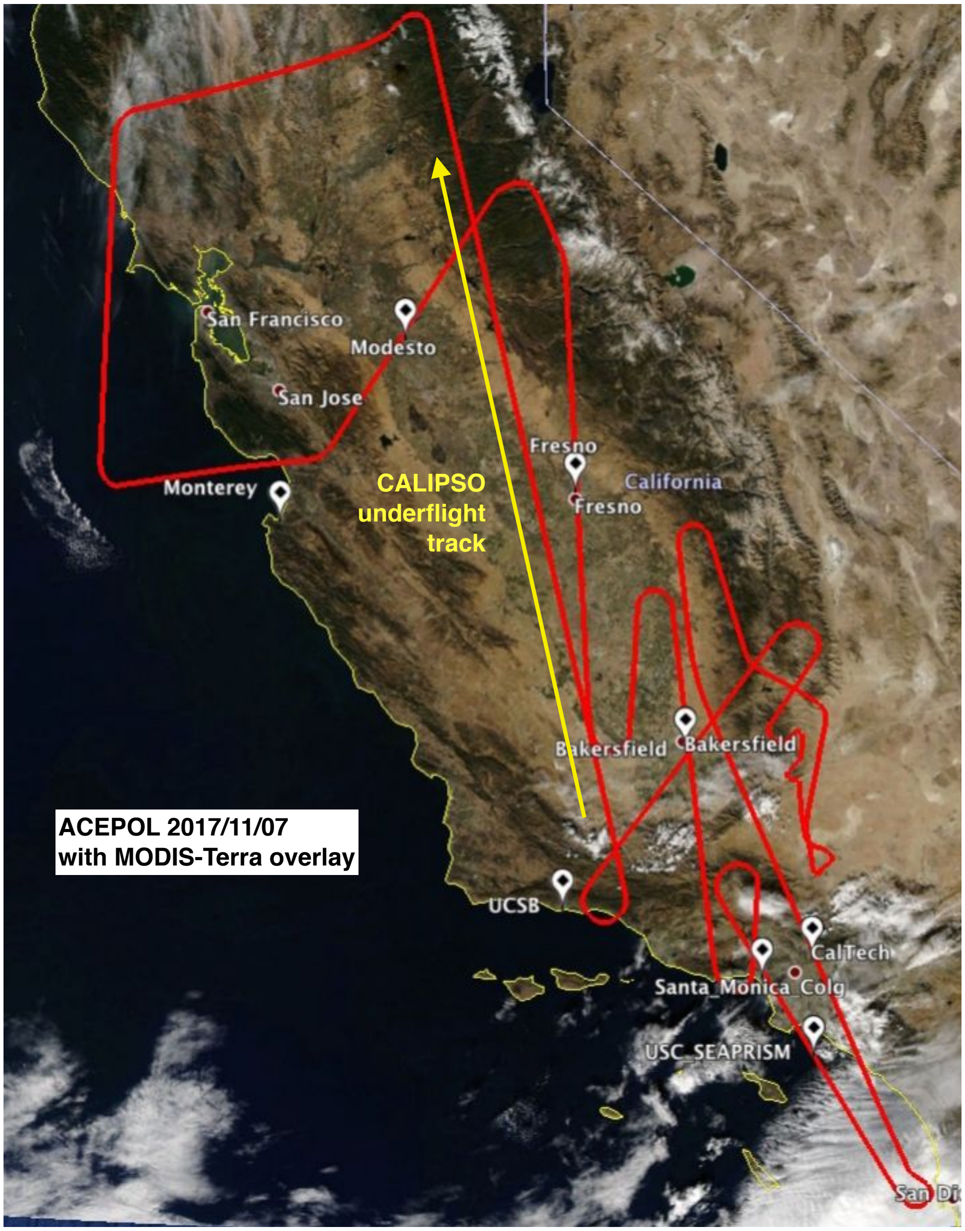

Figure 3 ACEPOL flight track coordinated with CALIPSO overflight. The flight track is in red, and the portion made in the CALIPSO track is indicated with the yellow arrow. The CALIPSO overflight time was 21:18 UTC, while the sample leg was started at 21:05 UTC and ended at 21:49 UTC. On this day AERONET sites (in white) and cirrus clouds to the southeast were also observed.

7.7 Data management plan

Data generated during the PACE-PAX will follow the NASA Earth Science Data and Information Policy (https://science.nasa.gov/earth-science/earth-science-data/data-information-policy/data-rights-related-issues) which requires data to be available from a designated long-term repository within a year of collection. Similar to other successful NASA campaigns, PACE-PAX will involve data manager from the early stages of planning to ultimately facilitate data submission and distribution.

Following the field deployment stage of PACE-PAX, we would like to hold one or several PACE-PAX data workshops. The goal of these workshops is to discuss the data that were collected during the field campaign, what was and was not accomplished, and how to access and analyze the data. We will also publish our results in a data journal, such as Earth System Science Data (https://www.earth-system-science-data.net/).

7.8 Risk assessment

Risk assessment is made in accordance with "NASA accepted Continuous Risk Management in accordance with NPR 7120.8D and NPR 8000.4" and held by the PACE-PAX PM, with input from MS, AM, WF.

#	Risk	Background	Response / Mitigation	Like-lihood	Consequence
A	PACE launch delay	PACE may launch later than expected.	Delay	2	3 Aircraft or instruments may not be available with delayed schedule. Optimal observation conditions may be missed.
B	PACE spacecraft failure	Full launch or spacecraft failure of the PACE mission.	Cancellation	1	5
C	Individual PACE instrument failure	Full individual instrument failure upon successful launch.	Descope of PACE-PAX	1	2 Fully planned validation mission would be descoped as described in previous sections, keeping the timeline so the optimal observation condition are captured.
D	PACE instrument data delivery delay	Fully calibrated data not available at the planned time point	Delay	2	3 Aircraft or instruments may not be available with delayed schedule. Optimal observation conditions may be missed.
E	Aircraft failure	Aircraft failure close to beginning or during PACE-PAX	Delay	2	4 (New) aircraft or instruments may not be available with delayed schedule. Optimal observation conditions may be missed.
F	Individual PACE-PAX instrument failure	An aircraft instrument in PACE-PAX fails to operate prior to or during the mission	Select instruments that have established successful heritage. Redundant observations.	2	2
G	Optimal observation conditions are not encountered	Measurement conditions required in the VTM are not encountered (for example,	Based on climatological assessments, estimate and provide sufficient margin on	3	1 VTM is organized for multiple objectives that rely on measurement conditions

		insufficient aerosol loads)	schedule and flight hours		
H	Unexpected extreme weather event(s)	Extreme environmental conditions along planned flight path or at BOP (e.g., hurricane, earthquake) result in extended suspension of flight operations	Modify/delay PACE-PAX plan	1	4

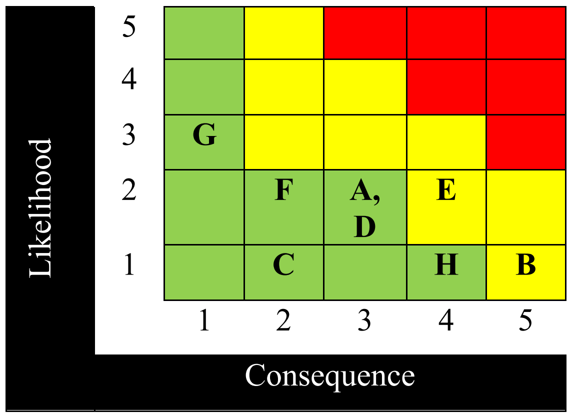

Figure 4 PACE-PAX risk matrix

7.9 Environmental impact planning

Something for the logistics team to complete
See: https://code200-external.gsfc.nasa.gov/250/environmental/environmental-planning-and-impact-assessment

7.10 Expectations for a safe fieldwork culture

To do

7.11 Connection with PACE Applications

To do ?

8 GUIDING FIELD CAMPAIGNS UNDERWAY

The success function, *S* (equation 5, defined in Section 4), is also a tool for planning an underway field campaign. It is used to help prioritize allocation of resources based upon the importance of validation objectives, completeness of the instrument suite, fulfillment of validation objectives thus far, and probability of future validation success. It identifies which of the measurement objectives will contribute the most to increasing the overall value of the success function. To do so, we consider the individual terms (each corresponding to a measurement objective) within the summation comprising *S*. More specifically, we identify the derivative of each measurement objective term with respect to time, *t*:

$$\frac{d}{dt_i}\left(S_i(t_i)\right) = c_i z_i \frac{p_i}{h_i} e^{-\frac{t_i p_i}{h_i}} \tag{6}$$

Note here that t_i now refers to observation of a specific measurement objective, and represents time spent *successfully* making observations that satisfy a measurement objective. Furthermore, p_i now represents probability of success specifically for the next increment of mission planning time, instead of for the duration of the mission.

This approach can be used, for example, for airborne field campaign flight planning by incorporating success thus far (t_i) and weather dependent probability of success in a subsequent day (p_i). To demonstrate, we use equation (6) to plan the Alpha theoretical field campaign. This is shown in Table 17.

The flight planning for day 1 of field campaign Alpha would use equation 6 to determine the success function derivative for each measurement objective. To start, we presume the probability of success is the same as was used in **Error! Reference source not found.**. In other words, the weather prediction is the same as climatology. Both measurement objectives A and B have identical high values of $S_i(t_i)'$. This is because they have equal probability of success, and because the greater weight of objective A is balanced by the smaller measurement time required for objective B. The decision, then, is to split the coming eight hour flight (a typical flight length) equally among both objectives.

Let us now presume that the flight on day 1 was successful, and four hours of measurements have been made for each of objective A and B. We take this into account for the assessment for day 2. Furthermore, the weather predictions have changed, along with the corresponding probability of success. Recalculation of $S_i(t_i)'$ compels us to devote the entirety of the flight on day 2 to objective D.

Now we assume that we were mostly successful on day 2 and made six hours of observations in an eight-hour flight. We have largely satisfied the time required for objective D, which is 5 hours, defined in equation 1 as the time required to satisfy the objective to 63%. If the weather stays the same for day 3, then our success function would direct us to refocus on measurement objective A, which has a lower probability of success but has thus far been less completely measured.

Table 17 Field campaign Alpha underway planning. This table illustrates how the derivative of the success function can be used to prioritize which measurement objectives to target on a given day, given weather (and other factor) driven probability of measurement success, plus information about the number of successful measurements have been made thus far. Boldfaced, white background values of $S_i(t_i)'$ indicate selected objectives for a given day.

Field campaign configuration				**Day 1**			**Day 2**			**Day 3**		
Meas. objective	**Weight, *w***	**Time required, *h***	**Completeness, *c***	t_i	**Prob. of success, *p***	$S_i(t_i)'$	t_i	**Prob. of success, *p***	$S_i(t_i)'$	t_i	**Prob. of success, *p***	$S_i(t_i)'$

A	4	20	1.0	0	0.50	**0.011**	**4**	0.50	0.010	4	0.50	**0.010**
B	2	10	1.0	0	0.50	**0.011**	**4**	0.50	0.009	4	0.50	0.009
C	2	15	0.0	0	0.10	0.0	0	0.75	0.0	0	0.75	0.0
D	1	5	1.0	0	0.10	0.002	0	0.75	**0.017**	**6**	0.75	0.007

In this manner, we can manage a field campaign that is underway, and account for measurements that have been made with varying probabilities of success. We have given an example for an airborne field campaign, for which decisions of measurement priority are complex, involve constantly changing and uncertain information (weather and other factors), and must be made rapidly. Sometimes, the weather or other conditions may be such that it is best not to perform a flight at all. In these cases, the values in $S_i(t_i)'$ would all be low. The decision to not perform a flight may depend on this and other factors, such as flight hours remaining, personnel, aircraft or other availability, and success thus far. As a metric to describe the latter, we define the mission completeness function, M:

$$M = \sum_{i=1}^{n} c_i z_i \left(1 - e^{-\frac{t_i}{h_i}}\right) \tag{7}$$

here t_i refers to the successful measurements for the ith objective thus far, and probability of success is not included. At the start of a field campaign, $M=0$, and it increases until $M=V$. If successful measurements have been made for times equal to the required observation time, h, for each objective, then M will have a value roughly 63.2% as large as V. If measurements have been made for three times h, then M will be 95% as large as V. In the example above, $M=0.153$ (19.8% of V) after the first day, and $M=0.2315$ (29.8% of V) after the second. This metric can be used to determine when a field campaign is 'done'. It roughly tracks the curve shown in Figure 1.

As previously noted, this approach has similarities with search and rescue theory described in Stone (1989) and elsewhere. In our case, each measurement objective can be considered a search area bin, and the corresponding elements of the success function derivative are a probability distribution function indicating the optimal bins in which to search. These are updated with subsequent measurements. As in any analysis incorporating subjective parameters, its realism depends upon how well these parameters were chosen. The benefit of these techniques is in their ability to break down complex conditions into simple assessments.

These tools will be used to perform flight planning during the operational phase of PACE-PAX. Flight planning will be aided by the "Moving Lines" software developed in Leblanc, 2018. This creates a flight path that can be submitted to the aircraft crew, which accounts for aircraft constraints, target location, solar geometry, (restricted) Special Use Areas (SUA), and other considerations.

Additionally, we expect to have one or more dry run flight planning activities in the months prior to PACE-PAX operations. The results of these activities can be assessed on how successfully measurement objectives would have been met had the aircraft flown that day.

9 STATISTICAL CONSIDERATIONS

Any measurement or retrieval includes some uncertainty, and any data collected represent only a sample of the real-world spatial and temporal covariation between the relevant geophysical parameters. Thus, the analysis of PACE-PAX (or any other) field campaign measurements is an inherently statistical enterprise, and the way that the data are compared, and which metrics are chosen to assess performance or consistency, are important and not necessarily the same for each geophysical quantity. Here we present some statistical considerations relevant to the eventual analysis of the data.

Traditionally, two data sets are often compared using a scatter plot, with linear ordinary least-squares regression metrics (such as fit intercept and slope, Pearson's correlation coefficient, and standard deviation or root mean square difference) reported to quantify agreement. However, this approach relies on a number of important assumptions which are often violated by our real-world geophysical data and applications, i.e., independent draws from the distribution of the true state; a linear model being the correct one to describe the relationship; a Gaussian distribution of deviations from the linear model; no uncertainty on the reference data or from the matchup technique (see discussion in Seegers *et al.*, 2018).

The violation of these assumptions has varying consequences in different situations. For example, small absolute uncertainties can nonetheless lead to a low Pearson correlation if the range of the parameter sampled is small. Or, if a retrieval performs very well but has one significant outlying failure case. Conversely, if a higher-uncertainty retrieval happens to sample an extreme outlier and recognize that it is an outlier (but misrepresent its magnitude) than a high correlation can be obtained. All of these situations arise because Pearson correlation is not a measure of agreement but rather of degree of linear covariation, with deviations penalized on a squared basis.

Uncertainties in the reference measurement and spatio-temporal variation are important, because these contribute to the discrepancy in the comparison but are not reflective of an actual error in the retrieval. Thus, a failure to account for them overstates the level of error in the data product being validated (Virtanen *et al.*, 2018; Sayer, 2020). This is a motivation for understanding the scales of variation of the data sampled in PACE-PAX (Objective 2 in Table 7). As a result, we propose the use of methods and metrics which account for the varying factors, which can affect the basic commonly reported validation metrics. Specifically, these methods include:

1. Ways to assess the consistency between reference and retrieval across the range of the parameter and in different conditions. Examples include the use of Bland-Altman assessment as an addition (or alternative) to scatter plots (Knobelspiesse *et al.*, 2019; McKinna *et al.*, 2021), and the subsetting of data into relevant subcategories, e.g., liquid vs. ice phase clouds, maritime vs. smoke-dominated aerosol loads, observations over land vs. Water (Sayer *et al.*, 2014).

2. Ways to assess uncertainty estimates reported by retrieval techniques (which are expected from most Project Science and SAT algorithms). These methods should account for the uncertainty in the reference data set (which is, in many cases, known) as well as the potential representativeness uncertainty introduced by spatiotemporal differences in the sampling of reference vs. Retrieval (Sayer, 2020; Sayer *et al.*, 2020).

3. Ways to assess to what extent the probability distribution function of retrieved quantities follows that observed by the airborne data (Platnick *et al.*, 2017; Sayer & Knobelspiesse, 2019), including relevant inter-parameter covariations if applicable (Marchand, 2013). This is relevant because many metrics (e.g., mean bias) only capture the overall bias tendency and do not reflect whether the variation in that parameter is reasonable (e.g., too wide or narrow, unrealistic skew/modes).

While methods may need to evolve dependent on the type and quality of data that are collected, the guiding principles are to, as far as possible, avoid, the use of analyses and metrics that are reliant on assumptions that may not be valid, and to validate the uncertainty model associated with a data product as well as the product itself. We acknowledge that a single field campaign cannot fully resolve all the above questions, but through achieving the Objectives listed in Table 7, it is expected that available capabilities and conditions should be sufficient to provide an understanding of performance over a variety of conditions.

10 CONCLUSIONS

The PACE-PAX field campaign is envisioned to meet the post-launch validation objectives of the PACE mission, especially those related to new products that cannot be met with the PVP alone. Because these objectives are varied, we have developed the VTM to show how validation objectives relate to measurement objectives, geophysical parameters, and mission requirements. We have also developed a scheme to qualitatively assign importance to individual objectives, along with other metrics that help in trade studies during mission design and flight planning during the campaign itself.

This document does not describe the details of the PACE-PAX mission itself. The complement of aircraft and instruments, choice of deployment region and length of study will be selected using the tools described here to stay within budget expectations. That said, the mission will probably look like an enhanced version of ACEPOL, which we have shown would have met many, but not all of PACE validation objectives had PACE been in orbit at that time.

11 ACRONYMS

4STAR	Spectrometer for Sky-Scanning Sun-Tracking Atmospheric Research
ACE	Aerosol-Cloud-Ecosystems
ACEPOL	Aerosol Characterization from Polarimeter and Lidar
AERONET	Aerosol Robotic Network
AFRC	NASA Armstrong Flight Research Center
AirMSPI	Airborne Multiangle SpectroPolarimetric Imager
AirHARP	Airborne version of Hyper-Angular Rainbow Polarimeter
AOD	Aerosol optical depth
ARC	Ames Research Center

AVIRIS-NG	Airborne Visible / Infrared Imaging Spectrometer – Next Generation
BST	Bayesian search theory
CALIPSO	Cloud-Aerosol Lidar and Infrared Pathfinder Satellite Observation
CAPS	Cloud Aerosol and Precipitation Spectrometer
CAS	Cloud and Aerosol Spectrometer
CATS	Cloud-Aerosol Transport System
CIP	Cloud Imaging Probe
CIRPAS	Center for Interdisciplinary Remotely Piloted Aircraft Studies
COD	Cloud optical depth
CPL	Cloud Physics Lidar
DoD	Department of Defense
FIREX-AQ	Fire Influence on Regional to Global Environments and Air Quality
FSSP	Forward Scattering Spectrometer Probe
GARP	Global Atmospheric Research Program
GISS	Goddard Institute for Space Studies
GSFC	Goddard Space Flight Center
HARP2	Hyper-Angular Rainbow Polarimeter 2
HQ	NASA Headquarters
HSRL-2	High Spectral Resolution Lidar – 2
ImPACT-PM	Imaging Polarimetric Assessment and Characterization of Tropospheric Particulate Matter
JPL	Jet Propulsion Laboratory
LACIE	Large Area Crop Inventory Experiment
LaRC	Langley Research Center
LARGE	Langley Aerosol Group Experiment
L1Cplan	PACE Level 1c data format
LWC	Liquid Water Content
MAIA	Multi-Angle Imager for Aerosols
MAN	Maritime Aerosol Network
MAP	Multi-angle, polarization sensitive
MAPP	Microphysical Aerosol Properties from Polarimetry
MarONet	Marine Optical Network
MAS	MODIS Airborne Simulator

MRD	Mission Requirements Document
MOBY	Marine Optical Buoy
MODIS	Moderate Resolution Imaging Spectroradiometer
NDBC	National Data Buoy Center
NPR	NASA Procedural Requirement
NOAA	National Oceanic Atmospheric Agency
NSF	National Science Foundation
OB	Operations Base
OCI	Ocean Color Instrument
ORACLES	ObseRvations of Aerosols above CLouds and their intEractionS
PACE	Plankton, Aerosol, Cloud, ocean Ecosystem
PACE-PAX	PACE Postlaunch Airborne eXperiment
PCASP	Passive Cavity Aerosol Spectrometer Probe
PVP	PACE Science Data Product Validation Plan
PVST	PACE Validation Science Team
PLRA	PACE Program Level Requirements Agreement
RSP	Research Scanning Polarimeter
SAM-CAAM	Systematic Aircraft Measurements to Characterize Aerosol Air Masses
SAT	PACE Science and Applications Team
SDPSL	PACE Science Data Product Selection Plan
SDS	PACE Project Science and Science Data Segments
SPEXone	Spectro-Polarimeter for Exploration, one
SPEX Airborne	Spectro-Polarimeter for Exploration, airborne
SRON	Netherlands Institute for Space Research
SSA	Aerosol single scattering albedo
STM	Science Traceability Matrix
SUA	Special Use Airspace
SVC	System vicarious calibration
SWIR	Shortwave infrared
TOA	Top of the Atmosphere
UMBC	University of Maryland, Baltimore County
UV	Ultraviolet
VIS	Visible

12 REFERENCES

Alexandrov, M. D., Cairns, B., Sinclair, K., Wasilewski, A. P., Ziemba, L., Crosbie, E., Moore, R., Hair, J., Scarino, A. J., Hu, Y., Stamnes, S., Shook, M. A., and Chen, G.: Retrievals of cloud droplet size from the research scanning polarimeter data: Validation using in situ measurements, Remote Sens. Environ., 210, 76 - 95, https://doi.org/10.1016/j.rse.2018.03.005, 2018.

Ansmann, A., Müller, D., Wandinger, U., and Mamouri, R. E.: Lidar profiling of aerosol optical and microphysical properties from space: overview, review, and outlook. in: First International Conference on Remote Sensing and Geoinformation of the Environment (RSCy2013) 1 -- 9) SPIE., doi: 10.1117/12.2028112, 2013.

Barnes, R.A., Eplee, R.E., Schmidt, G.M., Patt, F.S., McClain, C.R.: Calibration of SeaWiFS I Direct techniques. Appl. Opt. 40, 6682. https://doi.org/10.1364/ao.40.006682, 2001.

Bilstein, R. E.: Orders of Magnitude: A History of the NACA and NASA, 1915-1990, National Aeronautics and Space Administration, https://history.nasa.gov/SP-4406.pdf, 1989.

Bruegge, C. J., Arnold, G. T., Czapla-Myers, J., Dominguez, R., Helmlinger, M. C., Thompson, D. R., Van den Bosch, J., and Wenny, B. N.: Vicarious Calibration of eMAS, AirMSPI, and AVIRIS Sensors During FIREX-AQ, IEEE Transactions on Geoscience and Remote Sensing, 1-12, https://doi.org/10.1109/TGRS.2021.3066997, 2021.

Burton, S. P., Ferrare, R. A., Hostetler, C. A., Hair, J.W., Rogers, R. R., Obland, M. D., Butler, C. F., Cook, A. L., Harper, D. B., and Froyd, K. D.: Aerosol classification using airborne High Spectral Resolution Lidar measurements – methodology and examples, Atmos. Meas. Tech., 5, 73–98 https://doi.org/10.5194/amt-5-73-2012, 2012.

Burton, S. P., Hostetler, C. A., Cook, A. L., Hair, J. W., Seaman, S. T., Scola, S., Harper, D. B., Smith, J. A., Fenn, M. A., Ferrare, R. A., Saide, P. E., Chemyakin, E. V., and Müller, D.: Calibration of a high spectral resolution lidar using a Michelson interferometer, with data examples from ORACLES, Appl. Optics, 57, 6061–6075, 2018.

Cairns, B., E. Russell, E., and D. Travis, L. (1999). Research scanning polarimeter: calibration and ground-based measurements. Proc.SPIE 3754, 186–196. doi:10.1117/12.366329

Chapman, J. W., Thompson, D. R., Helmlinger, M. C., Bue, B. D., Green, R. O., Eastwood, M. L., Geier, S., Olson-Duvall, W., and Lundeen, S. R.: Spectral and Radiometric Calibration of the Next Generation Airborne Visible Infrared Spectrometer (AVIRIS-NG), Remote Sensing, 11(18), https://doi.org/10.3390/rs11182129, 2019.

Clark, D.K., Gordon, H.R., Voss, K.J., Ge, Y., Broenkow, W., Trees, C.: Validation of atmospheric correction over the oceans. J. Geophys. Res. Atmos. 102, 17209–17217. https://doi.org/10.1029/96JD03345, 1997.

Chiu, J. C., Marshak, A., Knyazikhin, Y., Wiscombe, W. J., Barker, H. W., Barnard, J. C., and Luo, Y.: Remote sensing of cloud properties using ground-based measurements of zenith radiance, J. Geophys. Res-Atmos., 111(D16), 2006.

Chiu, J. C., Huang, C.-H., Marshak, A., Slutsker, I., Giles, D. M., Holben, B. N., Knyazikhin, Y., and Wiscombe, W. J.: Cloud optical depth retrievals from the Aerosol Robotic Network (AERONET) cloud mode observations, J. Geophys. Res., 115(D14202), 2010.

Chowdhary, J., Cairns, B., and Travis, L.: Case Studies of Aerosol Retrievals over the Ocean from Multiangle, Multispectral Photopolarimetric Remote Sensing Data, J. Atmos. Sci., 59(3), 383--397, 2002.

Chowdhary, J., Cairns, B., Waquet, F., Knobelspiesse, K., Ottaviani, M., Redemann, J., Travis, L., and Mishchenko, M.: Sensitivity of multiangle, multispectral polarimetric remote sensing over open oceans to water-leaving radiance: Analyses of RSP data acquired during the MILAGRO campaign, Remote Sens. Environ., 118, 284--308, 2012.

Cox, C. and Munk, W.: Measurement of the roughness of the sea surface from photographs of the sun's glitter, Optical Society of America, 44(11), 1954.

Da Silva, A. M., Maring, H., Seidel, F., Behrenfeld, M., Ferrare, R., and Mace, G.: Aerosol, Cloud, Ecosystems (ACE) Final Study Report, National Aeronautics and Space Administration, https://ntrs.nasa.gov/, NASA/TP–20205007337, 2020.

Dickey, T., Lewis, M., and Chang, G.: Optical oceanography: Recent advances and future directions using global remote sensing and in situ observations, Reviews of Geophysics, 44(1), https://doi.org/https://doi.org/10.1029/2003RG000148, 2006.

Diner, D. J., Xu, F., Garay, M. J., Martonchik, J. V., Rheingans, B. E., Geier, S., Davis, A., Hancock, B. R., Jovanovic, V. M., Bull, M. A., Capraro, K., Chipman, R. A. and McClain, S. C. The Airborne Multiangle SpectroPolarimetric Imager (AirMSPI): a new tool for aerosol and cloud remote sensing, *Atmospheric Measurement Techniques,* 2013a, 6, 2007-2025

Diner, D. J., Garay, M. J., Kalashnikova, O. V., Rheingans, B. E., Geier, S., Bull, M. A., Jovanovic, V. M., Xu, F., Bruegge, C. J., Davis, A., and others: Airborne multiangle spectropolarimetric imager (AirMSPI) observations over California during NASA's polarimeter definition experiment (PODEX). in: SPIE Optical Engineering and Applications 88730B--88730B), 2013b.

Diner, D. J., Boland, S. W., Brauer, M., Bruegge, C., Burke, K. A., Chipman, R., Girolamo, L. D., Garay, M. J., Hasheminassab, S., Hyer, E., Jerrett, M., Jovanovic, V., Kalashnikova, O. V., Liu, Y., Lyapustin, A. I., Martin, R. V., Nastan, A., Ostro, B. D., Ritz, B., Schwartz, J., Wang, J., and Xu, F.: Advances in multiangle satellite remote sensing of speciated airborne particulate matter and association with adverse health effects: from MISR to MAIA, J. Appl. Remote Sens., 12(4), 1 -- 22, https://doi.org/10.1117/1.JRS.12.042603, 2018.

Dubovik, O. and King, M. D.: A flexible inversion algorithm for retrieval of aerosol optical properties from Sun and sky radiance measurements, J. Geophys. Res, 105, 20 673-20 696, 2000.

Dubovik, O., Holben, B., Eck, T. F., Smirnov, A., Kaufman, Y. J., King, M. D., Tanré, D., and Slutsker, I.: Variability of absorption and optical properties of key aerosol types observed in worldwide locations, J. Atmos. Sci., 59(3), 590--608, 2002.

Dubovik, O., Lapyonok, T., Litvinov, P., Herman, M., Fuertes, D., Ducos, F., Lopatin, A., Chaikovsky, A., Torres, B., Derimian, Y., and others: GRASP: a versatile algorithm for characterizing the atmosphere, SPIE(10.1117/2.1201408.005558), 2014.

Dubovik, O., Li, Z., Mishchenko, M. I., Tanre, D., Karol, Y., Bojkov, B., Cairns, B., Diner, D. J., Espinosa, W. R., Goloub, P., Gu, X., Hasekamp, O., Hong, J., Hou, W., Knobelspiesse, K. D., Landgraf, J., Li, L., Litvinov, P., Liu, Y., Lopatin, A., Marbach, T., Maring, H., Martins, V., Meijer, Y., Milinevsky, G., Mukai, S., Parol, F., Qiao, Y., Remer, L., Rietjens, J., Sano, I., Stammes, P., Stamnes, S., Sun, X., Tabary, P., Travis, L. D., Waquet, F., Xu, F., Yan, C., and Yin, D.: Polarimetric remote sensing of atmospheric aerosols: Instruments, methodologies, results, and perspectives, J. Quant. Spectrosc. Ra., 224, 474 - 511, https://doi.org/https://doi.org/10.1016/j.jqsrt.2018.11.024, 2019.

Dunagan, S. E., Johnson, R., Zavaleta, J., Russell, P. B., Schmid, B., Flynn, C., Redemann, J., Shinozuka, Y., Livingston, J., and Segal-Rosenhaimer, M.: Spectrometer for Sky-Scanning Sun-Tracking Atmospheric Research (4STAR): Instrument Technology, Remote Sensing, 5(8), 3872--3895, https://doi.org/10.3390/rs5083872, 2013.

Ellis, T. A., Myers, J., Grant, P., Platnick, S., Guerin, D. C., Fisher, J., Song, K., Kimchi, J., Kilmer, L., LaPorte, D. D., and Moeller, C. C.: The NASA enhanced MODIS airborne simulator. in: Earth Observing Systems XVI,https://doi.org/10.1117/12.894482, 2011234 -- 242) SPIE., 2011.

Eplee, R.E., Robinson, W.D., Bailey, S.W., Clark, D.K., Werdell, P.J., Wang, M., Barnes, R.A., McClain, C.R.: Calibration of SeaWiFS II Vicarious techniques. Appl. Opt. 40, 6701. https://doi.org/10.1364/ao.40.006701, 2001.

Faber, S., French, J. R., and Jackson, R.: Laboratory and in-flight evaluation of measurement uncertainties from a commercial Cloud Droplet Probe (CDP), Atmos. Meas. Tech., 11, 3645–3659, https://doi.org/10.5194/amt-11-3645-2018, 2018.

Fargion, G. S., Barnes, R., and McClain, C. R.: In Situ Aerosol Optical Thickness Collected by the SIMBIOS Program (1997-2000): Protocols, and Data QC and Analysis, National Aeronautical and Space administration Goddard Space Flight Space Center, NASA/TM-2001-209982, 2001.

Fox, D., Gonzalez, E., Kahn, R., and Martonchik, J.: Near-surface wind speed retrieval from space-based, multi-angle imaging of ocean Sun glint patterns, Remote Sens. Environ., 107(1), 223--231, 2007.

Franz, B.A., Bailey, S.W., Werdell, P.J., McClain, C.R.: Sensor-independent approach to the vicarious calibration of satellite ocean color radiometry. Appl. Opt. 46, 5068–5082. https://doi.org/10.1364/AO.46.005068., 2007.

Frouin, R. J., Franz, B. A., Ibrahim, A., Knobelspiesse, K., Ahmad, Z., Cairns, B., Chowdhary, J., Dierssen, H. M., Tan, J., Dubovik, O., Huang, X., Davis, A. B., Kalashnikova, O., Thompson, D. R., Remer, L. A., Boss, E., Coddington, O., Deschamps, P.-Y., Gao, B.-C., Gross, L., Hasekamp, O., Omar, A., Pelletier, B., Ramon, D., Steinmetz, F., and Zhai, P.-W.: Atmospheric Correction of Satellite Ocean-Color Imagery During the PACE Era, Frontiers in Earth Science, 7, 145 , https://doi.org/10.3389/feart.2019.00145, 2019.

Fu, G., Hasekamp, O., Rietjens, J., Smit, M., Di Noia, A., Cairns, B., Wasilewski, A., Diner, D., Xu, F., Knobelspiesse, K., Gao, M., da Silva, A., Burton, S., Hostetler, C., Hair, J., and Ferrare, R.: Aerosol retrievals from the ACEPOL Campaign, Atmos. Meas. Tech. Discuss., 2019, 1--30, https://doi.org/10.5194/amt-2019-287, 2019.

Gao, M., Zhai, P.-W., Franz, B. A., Hu, Y., Knobelspiesse, K., Werdell, P. J., Ibrahim, A., Cairns, B., and Chase, A.: Inversion of multiangular polarimetric measurements over open and coastal ocean waters: a joint retrieval algorithm for aerosol and water-leaving radiance properties, Atmos. Meas. Tech., 12(7), 3921--3941, https://doi.org/10.5194/amt-12-3921-2019, 2019.

Gao, M., Zhai, P.-W., Franz, B. A., Knobelspiesse, K., Ibrahim, A., Cairns, B., Craig, S. E., Fu, G., Hasekamp, O., Hu, Y., and Werdell, P. J.: Inversion of multiangular polarimetric measurements from the ACEPOL campaign: an application of improving aerosol property and hyperspectral ocean color retrievals, Atmospheric Measurement Techniques, 13(7), 3939--3956, https://doi.org/10.5194/amt-13-3939-2020, 2020.

Gao, M., Franz, B. A., Knobelspiesse, K., Zhai, P.-W., Martins, V., Burton, S., Cairns, B., Ferrare, R., Gales, J., Hasekamp, O., Hu, Y., Ibrahim, A., McBride, B., Puthukkudy, A., Werdell, P. J., and Xu, X.: Efficient multi-angle polarimetric inversion of aerosols and ocean color powered by a deep neural network forward model, Atmospheric Measurement Techniques Discussions, 2021, 1--41 , https://doi.org/10.5194/amt-2020-507, 2021.

Giles, D. M., Sinyuk, A., Sorokin, M. G., Schafer, J. S., Smirnov, A., Slutsker, I., Eck, T. F., Holben, B. N., Lewis, J. R., Campbell, J. R., Welton, E. J., Korkin, S. V., and Lyapustin, A. I.: Advancements in the Aerosol Robotic Network (AERONET) Version~3 database -- automated near-real-time quality control algorithm with improved cloud screening for Sun photometer aerosol optical depth (AOD) measurements, Atmospheric Measurement Techniques, 12(1), 169--209, https://doi.org/10.5194/amt-12-169-2019, 2019.

Hair, J. W., Hostetler, C. A., Cook, A. L., Harper, D. B., Ferrare, R. A., Mack, T. L., Welch, W., Izquierdo, L. R., and Hovis, F. E.: Airborne High Spectral Resolution Lidar for profiling aerosol optical properties, Appl. Optics, 47, 6734–6752, 2008.

Hannadige, N. K., Zhai, P.-W., Gao, M., Franz, B. A., Hu, Y., Knobelspiesse, K., Werdell, P. J., Ibrahim, A., Cairns, B., and Hasekamp, O. P.: Atmospheric correction over the ocean for hyperspectral radiometers using multi-angle polarimetric retrievals, Opt. Express, 29(3), 4504--4522, https://doi.org/10.1364/OE.408467, 2021.

Hasekamp, O. P. and Landgraf, J.: Retrieval of aerosol properties over the ocean from multispectral single-viewing-angle measurements of intensity and polarization: Retrieval approach, information content, and sensitivity study, J. Geophys. Res, 110, D20207, 2005.

Hasekamp, O. P., Litvinov, P., and Butz, A.: Aerosol properties over the ocean from PARASOL multiangle photopolarimetric measurements, J. Geophys. Res, 116(D14), D14204, 2011.

Hasekamp, O. P., Fu, G., Rusli, S. P., Wu, L., Noia, A. D., aan de Brugh, J., Landgraf, J., Smit, J. M., Rietjens, J., and van Amerongen, A.: Aerosol measurements by SPEXone on the NASA PACE mission: expected retrieval capabilities, J. Quant. Spectrosc. Ra., 227, 170 - 184, https://doi.org/https://doi.org/10.1016/j.jqsrt.2019.02.006, 2019.

Hlavka, D. L., Yorks, J. E., Young, S. A., Vaughan, M. A., Kuehn, R. E., McGill, M. J., and Rodier, S. D.: Airborne validation of cirrus cloud properties derived from CALIPSO lidar measurements: Optical properties, J. Geophys. Res-Atmos., 117(D9), 2012.

Hoge, F. E. and Swift, R. N.: Application of the NASA airborne oceanographic lidar to the mapping of chlorophyll and other organic pigments, National Aeronautics and Space Administration, https://ntrs.nasa.gov/citations/19820002811, 1981.

Holben, B. N., Eck, T. F., Slutsker, I., Tanré, D., Buis, J. P., Setzer, A., Vermote, E., Reagan, J. A., Kaufman, Y. J., Nakajima, T., Lavenu, F., Jankowiak, I., and Smirnov, A.: AERONET---A Federated Instrument Network and Data Archive for Aerosol Characterization, Remote Sens. Environ., 66(1), 1 - 16, https://doi.org/https://doi.org/10.1016/S0034-4257(98)00031-5, 1998.

Hsu, N. C., Jeong, M.-J., Bettenhausen, C., Sayer, A. M., Hansell, R., Seftor, C. S., Huang, J., and Tsay, S.-C.: Enhanced Deep Blue aerosol retrieval algorithm: The second generation, J. Geophys. Res-Atmos., 118(16), 9296--9315, https://doi.org/10.1002/jgrd.50712, 2013.

Ibrahim, A., Franz, B.A., Ahmad, Z., Bailey, S.W.: Multiband Atmospheric Correction Algorithm for Ocean Color Retrievals. Front. Earth Sci. 7. https://doi.org/10.3389/feart.2019.00116., 2019.

Jamet, C., Ibrahim, A., Ahmad, Z., Angelini, F., Babin, M., Behrenfeld, M. J., Boss, E., Cairns, B., Churnside, J., Chowdhary, J., Davis, A. B., Dionisi, D., Duforêt-Gaurier, L., Franz, B., Frouin, R., Gao, M., Gray, D., Hasekamp, O., He, X., Hostetler, C., Kalashnikova, O. V., Knobelspiesse, K., Lacour, L., Loisel, H., Martins, V., Rehm, E., Remer, L., Sanhaj, I., Stamnes, K., Stamnes, S., Victori, S., Werdell, J., and Zhai, P.-W.: Going Beyond Standard Ocean Color Observations: Lidar and Polarimetry, Frontiers in Marine Science, 6, 251 , https://doi.org/10.3389/fmars.2019.00251, 2019.

Kahn, R. A., Berkoff, T. A., Brock, C., Chen, G., Ferrare, R. A., Ghan, S., Hansico, T. F., Hegg, D. A., Martins, J. V., McNaughton, C. S., and others: SAM-CAAM: A Concept for Acquiring

Systematic Aircraft Measurements to Characterize Aerosol Air Masses, B. Am. Meteorol. Soc., 98(10), 2215--2228, 2017.

Kalashnikova, O. V., Garay, M. J., Bates, K. H., Kenseth, C. M., Kong, W., Cappa, C. D., Lyapustin, A. I., Jonsson, H. H., Seidel, F. C., Xu, F., Diner, D. J., and Seinfeld, J. H.: Photopolarimetric Sensitivity to Black Carbon Content of Wildfire Smoke: Results From the 2016 ImPACT-PM Field Campaign, J. Geophys. Res-Atmos., 123(10), 5376-5396, https://doi.org/10.1029/2017JD028032, 2018.

Kassianov, E., Flynn, C., Redemann, J., Schmid, B., Russell, P. B., and Sinyuk, A.: Initial Assessment of the Spectrometer for Sky-Scanning, Sun-Tracking Atmospheric Research (4STAR)-Based Aerosol Retrieval: Sensitivity Study, Atmosphere, 3(4), 495--521, 2012.

King, M. D., Menzel, W. P., Grant, P. S., Myers, J. S., Arnold, G. T., Platnick, S. E., Gumley, L. E., Tsay, S.-C., Moeller, C. C., Fitzgerald, M., Brown, K. S., and Osterwisch, F. G.: Airborne Scanning Spectrometer for Remote Sensing of Cloud, Aerosol, Water Vapor, and Surface Properties, Journal of Atmospheric and Oceanic Technology, 13(4), 777 - 794, https://doi.org/10.1175/1520-0426(1996)013<0777:ASSFRS>2.0.CO;2, 1996.

Knobelspiesse, K., Cairns, B., Ottaviani, M., Ferrare, R., Hair, J., Hostetler, C., Obland, M., Rogers, R., Redemann, J., Shinozuka, Y., Clarke, A., Freitag, S., Howell, S., Kapustin, V., and McNaughton, C.: Combined retrievals of boreal forest fire aerosol properties with a polarimeter and lidar, Atmos. Chem. Phys., 11, 7045--7067, https://doi.org/10.5194/acp-11-7045-2011, 2011a.

Knobelspiesse, K., Cairns, B., Redemann, J., Bergstrom, R. W., and Stohl, A.: Simultaneous retrieval of aerosol and cloud properties during the MILAGRO field campaign, Atmos. Chem. Phys., 11, 6245-6263, https://doi.org/10.5194/acp-11-6245-2011, 2011b.

Knobelspiesse, K., Cairns, B., Mishchenko, M., Chowdhary, J., Tsigaridis, K., van Diedenhoven, B., Martin, W., Ottaviani, M., and Alexandrov, M.: Analysis of fine-mode aerosol retrieval capabilities by different passive remote sensing instrument designs, Opt. Express, 20(19), 21457-21484, 2012.

Knobelspiesse, K. and Nag, S.: Remote sensing of aerosols with small satellites in formation flight, Atmos. Meas. Tech., 11(7), 3935--3954, https://doi.org/10.5194/amt-11-3935-2018, 2018.

Knobelspiesse, K., Tan, Q., Bruegge, C., Cairns, B., Chowdhary, J., van Diedenhoven, B., et al.: Intercomparison of airborne multi-angle polarimeter observations from the Polarimeter Definition Experiment. Applied Optics, 58(3), 650–669. https://doi.org/10.1364/AO.58.000650, 2019.

Knobelspiesse, K., Barbosa, H. M. J., Bradley, C., Bruegge, C., Cairns, B., Chen, G., Chowdhary, J., Cook, A., Di Noia, A., van Diedenhoven, B., Diner, D. J., Ferrare, R., Fu, G., Gao, M., Garay, M., Hair, J., Harper, D., van Harten, G., Hasekamp, O., Helmlinger, M., Hostetler, C., Kalashnikova, O., Kupchock, A., Longo De Freitas, K., Maring, H., Martins, J. V., McBride, B., McGill, M., Norlin, K., Puthukkudy, A., Rheingans, B., Rietjens, J., Seidel, F. C., da Silva, A., Smit, M., Stamnes, S., Tan, Q., Val, S., Wasilewski, A., Xu, F., Xu, X., and Yorks, J.: The Aerosol

Characterization from Polarimeter and Lidar (ACEPOL) airborne field campaign, Earth System Science Data, 12(3), 2183--2208 , https://doi.org/10.5194/essd-12-2183-2020, 2020.

Knobelspiesse, K., Ibrahim, A., Franz, B., Bailey, S., Levy, R., Ahmad, Z., Gales, J., Gao, M., Garay, M., Anderson, S., and Kalashnikova, O.: Analysis of simultaneous aerosol and ocean glint retrieval using multi-angle observations, Atmospheric Measurement Techniques, 14(5), 3233--3252, https://doi.org/10.5194/amt-14-3233-2021, 2021.

LeBlanc, S. (2018, November 5). samuelleblanc/fp: Moving Lines: NASA airborne research flight planning tool release (Version v1.21). Zenodo. http://doi.org/10.5281/zenodo.1478126

Lee, C. M., Cable, M. L., Hook, S. J., Green, R. O., Ustin, S. L., Mandl, D. J., and Middleton, E. M.: An introduction to the NASA Hyperspectral InfraRed Imager (HyspIRI) mission and preparatory activities, Remote Sensing of Environment, 167, 6-19, https://doi.org/https://doi.org/10.1016/j.rse.2015.06.012, 2015.

MacDonald, R. B.: Large Area Crop Inventory Experiment (LACIE) Phase II Evaluation Report, National Aeronautics and Space Administration, https://ntrs.nasa.gov/api/citations/19770024640/downloads/19770024640.pdf, 1977.

Marchand, R.: Trends in ISCCP, MISR, and MODIS cloud-top-height and optical-depth histograms, J. Geophys. Res. Atmos., 118, 1941– 1949, https://doi.org/10.1002/jgrd.50207, 2013.

Marshak, A., Knyazikhin, Y., Evans, K. D., and Wiscombe, W. J.: The ``RED versus NIR'' plane to retrieve broken-cloud optical depth from ground-based measurements, J. Atmos. Sci., 61(15), 1911--1925, 2004.

Martins, J. V., Fernandez-Borda, R., McBride, B., Remer, L., and Barbosa, H. M.: The HARP Hyperangular Imaging Polarimeter and the Need for Small Satellite Payloads with High Science Payoff for Earth Science Remote Sensing. in: IGARSS 2018-2018 IEEE International Geoscience and Remote Sensing Symposium 6304--6307), 2018.

McBride, B. A., Martins, J. V., Barbosa, H. M., Birmingham, W., and Remer, L. A.: Spatial distribution of cloud droplet size properties from Airborne Hyper-Angular Rainbow Polarimeter (AirHARP) measurements, Atmos. Meas. Tech., 13(4), 1777--1796, 2020.

McGill, M., Hlavka, D., Hart, W., Scott, V. S., Spinhirne, J., and Schmid, B.: Cloud Physics Lidar: instrument description and initial measurement results, Appl. Optics, 41(18), 3725--3734, https://doi.org/10.1364/AO.41.003725, 2002.

McGill, M. J., Vaughan, M. A., Trepte, C. R., Hart, W. D., Hlavka, D. L., Winker, D. M., and Kuehn, R.: Airborne validation of spatial properties measured by the CALIPSO lidar, J. Geophys. Res-Atmos., 112(D20), 2007.

McGill, M. J., Yorks, J. E., Scott, V. S., Kupchock, A. W., and Selmer, P. A.: The Cloud-Aerosol Transport System (CATS): A technology demonstration on the International Space Station. in: Lidar Remote Sensing for Environmental Monitoring XV 96120A), 2015.

McKinna, L. I. W., Cetinić, I., & Werdell, P. J.: Development and validation of an empirical ocean color algorithm with uncertainties: A case study with the particulate backscattering coefficient, Journal of Geophysical Research: Oceans, 126, e2021JC017231, https://doi.org/10.1029/2021JC017231, 2021

Mishchenko, M. I., Cairns, B., Hansen, J. E., Travis, L. D., Burg, R., Kaufman, Y. J., Vanderlei Martins, J., and Shettle, E. P.: Monitoring of aerosol forcing of climate from space: analysis of measurement requirements, J. Quant. Spectrosc. Ra., 88(1-3), 149--161, 2004.

Mouroulis, P., Van Gorp, B., Green, R. O., Dierssen, H., Wilson, D. W., Eastwood, M., Boardman, J., Gao, B.-C., Cohen, D., Franklin, B., and others: Portable Remote Imaging Spectrometer coastal ocean sensor: design, characteristics, and first flight results, Appl. Optics, 53(7), 1363--1380, 2014.

J. L. Mueller, Clark, D.K., Kuwahara, V.S., Lazin, G., Brown, S.W., Fargion, G.S., Yarbrough, M.A., Feinholz, M., Flora, S., Broenkow, W., Kim, Y.S., Johnson, B.C., Yuen, M., Strutton, P.G., Dickey, T.D., Abbott, M.R., Letelier, R.M., Lewis, M.R., McLean, S., Chavez, F.P., Barnard, A., Morrison, J.R., Subramaniam, A., Manov, D., Zheng, X., Harding, L.W.J., Barnes, R.A., Lykke, K.R.: Ocean Optics Protocols For Satellite Ocean Color Sensor Validation, Revision 4, Volume VI: Special Topics in Ocean Optics Protocols and Appendice. Greenbelt, Maryland, USA., 2003.

Müller, D., Hostetler, C. A., Ferrare, R. A., Burton, S. P., Chemyakin, E., Kolgotin, A., Hair, J. W., Cook, A. L., Harper, D. B., Rogers, R. R., Hare, R. W., Cleckner, C. S., Obland, M. D., Tomlinson, J., Berg, L. K., and Schmid, B.: Airborne Multiwavelength High Spectral Resolution Lidar (HSRL-2) observations during TCAP 2012: vertical profiles of optical and microphysical properties of a smoke/urban haze plume over the northeastern coast of the US, Atmos. Meas. Tech., 7, 3487–3496, https://doi.org/10.5194/amt-7-3487-2014, 2014.

National Academies of Sciences, Engineering, and Medicine. 2018. Thriving on Our Changing Planet: A Decadal Strategy for Earth Observation from Space. Washington, DC: The National Academies Press. https://doi.org.10.17226/24938.

Ottaviani, M., Foster, R., Gilerson, A., Ibrahim, A., Carrizo, C., El-Habashi, A., Cairns, B., Chowdhary, J., Hostetler, C., Hair, J., Burton, S., Hu, Y., Twardowski, M., Stockley, N., Gray, D., Slade, W., and Cetinic, I.: Airborne and shipborne polarimetric measurements over open ocean and coastal waters: Intercomparisons and implications for spaceborne observations, Remote Sens. Environ., 206, 375 - 390 , https://doi.org/https://doi.org/10.1016/j.rse.2017.12.015, 2018.

Perry, J. S.: The Global Atmospheric Research Program, Reviews of Geophysics, 13(3), 661-667, https://doi.org/https://doi.org/10.1029/RG013i003p00661, 1975.

Platnick, S., Meyer, K. G., King, M. D., Wind, G., Amarasinghe, N., Marchant, B., Arnold, G. T., Zhang, Z., Hubanks, P. A., Holz, R. E., Yang, P., Ridgway, W. L., and Riedi, J: The MODIS Cloud Optical and Microphysical Products: Collection 6 Updates and Examples From Terra and Aqua, IEEE Trans. Geosci. Remote Sens., 55(1), 502-525, https://doi.org/10.1109/TGRS.2016.2610522, 2017.

Puthukkudy, A., Martins, J. V., Remer, L. A., Xu, X., Dubovik, O., Litvinov, P., McBride, B., Burton, S., and Barbosa, H. M. J.: Retrieval of aerosol properties from Airborne Hyper-Angular Rainbow Polarimeter (AirHARP) observations during ACEPOL 2017, Atmospheric Measurement Techniques, 13(10), 5207--5236, https://doi.org/10.5194/amt-13-5207-2020, 2020.

Redemann, J., Wood, R., Zuidema, P., Doherty, S. J., Luna, B., LeBlanc, S. E., Diamond, M. S., Shinozuka, Y., Chang, I. Y., Ueyama, R., Pfister, L., Ryoo, J.-M., Dobracki, A. N., da Silva, A. M., Longo, K. M., Kacenelenbogen, M. S., Flynn, C. J., Pistone, K., Knox, N. M., Piketh, S. J., Haywood, J. M., Formenti, P., Mallet, M., Stier, P., Ackerman, A. S., Bauer, S. E., Fridlind, A. M., Carmichael, G. R., Saide, P. E., Ferrada, G. A., Howell, S. G., Freitag, S., Cairns, B., Holben, B. N., Knobelspiesse, K. D., Tanelli, S., L'Ecuyer, T. S., Dzambo, A. M., Sy, O. O., McFarquhar, G. M., Poellot, M. R., Gupta, S., O'Brien, J. R., Nenes, A., Kacarab, M., Wong, J. P. S., Small-Griswold, J. D., Thornhill, K. L., Noone, D., Podolske, J. R., Schmidt, K. S., Pilewskie, P., Chen, H., Cochrane, S. P., Sedlacek, A. J., Lang, T. J., Stith, E., Segal-Rozenhaimer, M., Ferrare, R. A., Burton, S. P., Hostetler, C. A., Diner, D. J., Seidel, F. C., Platnick, S. E., Myers, J. S., Meyer, K. G., Spangenberg, D. A., Maring, H., and Gao, L.: An overview of the ORACLES (ObseRvations of Aerosols above CLouds and their intEractionS) project: aerosol--cloud--radiation interactions in the southeast Atlantic basin, Atmospheric Chemistry and Physics, 21(3), 1507--1563, https://doi.org/10.5194/acp-21-1507-2021, 2021.

Sayer, A. M., Munchak, L. A., Hsu, N. C., Levy, R. C., Bettenhausen, C., and Jeong, M.-J.: MODIS Collection 6 aerosol products: Comparison between Aqua's e-Deep Blue, Dark Target, and “merged” data sets, and usage recommendations, J. Geophys. Res. Atmos., 119, 13,965–13,989, https://doi.org/10.1002/2014JD022453, 2014.

Sayer, A. M. and Knobelspiesse, K. D.: How should we aggregate data? Methods accounting for the numerical distributions, with an assessment of aerosol optical depth, Atmos. Chem. Phys., 19, 15023–15048, https://doi.org/10.5194/acp-19-15023-2019, 2019.

Sayer, A. M.: How long is too long? Variogram analysis of AERONET data to aid aerosol validation and intercomparison studies. Earth and Space Science, 7, e2020EA001290. https://doi.org/10.1029/2020EA001290, 2020.

Sayer, A. M., Govaerts, Y., Kolmonen, P., Lipponen, A., Luffarelli, M., Mielonen, T., Patadia, F., Popp, T., Povey, A. C., Stebel, K., and Witek, M. L.: A review and framework for the evaluation of pixel-level uncertainty estimates in satellite aerosol remote sensing, Atmos. Meas. Tech., 13, 373–404, https://doi.org/10.5194/amt-13-373-2020, 2020.

Sawamura, P., Moore, R. H., Burton, S. P., Chemyakin, E., Müller, D., Kolgotin, A., Ferrare, R. A., Hostetler, C. A., Ziemba, L. D., Beyersdorf, A. J., and Anderson, B. E.: HSRL-2 aerosol optical measurements and microphysical retrievals vs. Airborne in situ measurements during DISCOVER-AQ 2013: an intercomparison study, Atmos. Chem. Phys., 17, 7229–7243, https://doi.org/10.5194/acp-17-7229-2017, 2017.

Scarino, A. J., Obland, M. D., Fast, J. D., Burton, S. P., Ferrare, R. A., Hostetler, C. A., Berg, L. K., Lefer, B., Haman, C., Hair, J. W., Rogers, R. R., Butler, C., Cook, A. L., and Harper, D. B.: Comparison of mixed layer heights from airborne high spectral resolution lidar, ground-based measurements, and the WRF-Chem model during CalNex and CARES, Atmos. Chem. Phys., 14, 5547–5560, https://doi.org/10.5194/acp-14-5547-2014, 2014.

Schafer, J. S., Eck, T. F., Holben, B. N., Thornhill, K. L., Ziemba, L. D., Sawamura, P., Moore, R. H., Slutsker, I., Anderson, B. E., Sinyuk, A., Giles, D. M., Smirnov, A., Beyersdorf, A. J., and Winstead, E. L.: Intercomparison of aerosol volume size distributions derived from AERONET ground-based remote sensing and LARGE in situ aircraft profiles during the 2011--2014 DRAGON and DISCOVER-AQ experiments, Atmospheric Measurement Techniques, 12(10), 5289--5301, https://doi.org/10.5194/amt-12-5289-2019, 2019.

Seegers, B. N., Stumpf, R. P., Schaeffer, B. A., Loftin K. A., and Werdell, P. J.: Performance metrics for the assessment of satellite data products: an ocean color case study, Opt. Express 26, 7404-7422, https://doi.org/10.1364/OE.26.007404, 2018

Sellers, B., Hunderwadel, J. L., and Hanser, F. A.: Flight of a UV spectrophotometer aboard Galileo 2, the NASA Convair 990 aircraft, Office of Naval Research, https://ntrs.nasa.gov/citations/19760024408, 1976.

Shinozuka, Y., Clarke, A. D., Howell, S. G., Kapustin, V. N., McNaughton, C. S., Zhou, J., and Anderson, B. E.: {Aircraft profiles of aerosol microphysics and optical properties over North America: Aerosol optical depth and its association with PM2. 5 and water uptake}, J. Geophys. Res-Atmos., 112(D12), D12S20, 2007.

Shinozuka, Y., Redemann, J., Livingston, J., Russell, P., Clarke, A., Howell, S., Freitag, S., O'Neill, N., Reid, E., Johnson, R., and others: {Airborne observation of aerosol optical depth during ARCTAS: vertical profiles, inter-comparison, fine-mode fraction and horizontal variability}, Atmos. Chem. Phys. Discuss., 10, 18315-18363, 2010.

Shipley, S. T., Tracy, D. H., Eloranta, E. W., Trauger, J. T., Sroga, J. T., Roesler, F. L., and Weinman, J. A.: High spectral resolution lidar to measure optical scattering properties of atmospheric aerosols. 1: Theory and instrumentation, Appl. Opt., 22(23), 3716--3724, https://doi.org/10.1364/AO.22.003716, 1983.

Siegel, D. A., Buesseler, K. O., Behrenfeld, M. J., Benitez-Nelson, C. R., Boss, E., Brzezinski, M. A., Burd, A., Carlson, C. A., D'Asaro, E. A., Doney, S. C., Perry, M. J., Stanley, R. H. R., and Steinberg, D. K.: Prediction of the Export and Fate of Global Ocean Net Primary Production: The EXPORTS Science Plan, Frontiers in Marine Science, 3, 22 , https://doi.org/10.3389/fmars.2016.00022, 2016.

Siegel, D. A., Cetinić, I., Graff, J. R., Lee, C. M., Nelson, N., Perry, M. J., Ramos, I. S., Steinberg, D. K., Buesseler, K., Hamme, R., Fassbender, A. J., Nicholson, D., Omand, M. M., Robert, M., Thompson, A., Amaral, V., Behrenfeld, M., Benitez-Nelson, C., Bisson, K., Boss, E., Boyd, P. W., Brzezinski, M., Buck, K., Burd, A., Burns, S., Caprara, S., Carlson, C., Cassar, N., Close, H., D'Asaro, E., Durkin, C., Erickson, Z., Estapa, M. L., Fields, E., Fox, J., Freeman, S., Gifford, S., Gong, W., Gray, D., Guidi, L., Haëntjens, N., Halsey, K., Huot, Y., Hansell, D., Jenkins, B., Karp-Boss, L., Kramer, S., Lam, P., Lee, J.-M., Maas, A., Marchal, O., Marchetti, A., McDonnell, A., McNair, H., Menden-Deuer, S., Morison, F., Niebergall, A. K., Passow, U., Popp, B., Potvin, G., Resplandy, L., Roca-Martí, M., Roesler, C., Rynearson, T., Traylor, S., Santoro, A., Seraphin, K. D., Sosik, H. M., Stamieszkin, K., Stephens, B., Tang, W., Van Mooy, B., Xiong, Y., and Zhang, X.: An operational overview of the EXport Processes in the Ocean from RemoTe Sensing (EXPORTS) Northeast Pacific field deployment, Elementa: Science of the Anthropocene, 9(1) , https://doi.org/10.1525/elementa.2020.00107, 2021.

Sinyuk, A., Holben, B. N., Eck, T. F., Giles, D. M., Slutsker, I., Korkin, S., Schafer, J. S., Smirnov, A., Sorokin, M., and Lyapustin, A.: The AERONET Version 3 aerosol retrieval algorithm, associated uncertainties and comparisons to Version 2, Atmospheric Measurement Techniques, 13(6), 3375--3411, https://doi.org/10.5194/amt-13-3375-2020, 2020.

Small III, A. A., Stefik, J. B., Verlinde, J., and Johnson, N. C.: The cloud hunter's problem: An automated decision algorithm to improve the productivity of scientific data collection in stochastic environments, Monthly weather review, 139(7), 2276--2289, 2011.

Smirnov, A., Holben, B. N., Slutsker, I., Giles, D. M., McClain, C. R., Eck, T. F., Sakerin, S. M., Macke, A., Croot, P., Zibordi, G., Quinn, P. K., Sciare, J., Kinne, S., Harvey, M., Smyth, T. J., Piketh, S., Zielinski, T., Proshutinsky, A., Goes, J. I., Nelson, N. B., Larouche, P., Radionov, V. F., Goloub, P., Moorthy, K. K., Matarrese, R., Robertson, E. J., and Jourdin, F.: Maritime Aerosol Network as a component of Aerosol Robotic Network, J. Geophys. Res., 114(D06204), 2009.

Smit, J. M., Rietjens, J. H., di Noia, A., Hasekamp, O. P., Laauwen, W., Cairns, B., van Diedenhoven, B., and Wasilewski, A.: In-flight validation of SPEX airborne spectro-polarimeter onboard NASA's research aircraft ER-2. in: International Conference on Space Optics---ICSO 2018 111800N), 2019a.

Smit, J. M., Rietjens, J. H. H., van Harten, G., Noia, A. D., Laauwen, W., Rheingans, B. E., Diner, D. J., Cairns, B., Wasilewski, A., Knobelspiesse, K. D., Ferrare, R., and Hasekamp, O. P.: SPEX airborne spectropolarimeter calibration and performance, Appl. Optics, 58(21), 5695--5719, https://doi.org/10.1364/AO.58.005695, 2019b.

Sorooshian, A., Anderson, B., Bauer, S. E., Braun, R. A., Cairns, B., Crosbie, E., Dadashazar, H., Diskin, G., Ferrare, R., Flagan, R. C., Hair, J., Hostetler, C., Jonsson, H. H., Kleb, M. M., Liu, H., MacDonald, A. B., McComiskey, A., Moore, R., Painemal, D., Russell, L. M., Seinfeld, J. H., Shook, M., Smith, W. L., Thornhill, K., Tselioudis, G., Wang, H., Zeng, X., Zhang, B., Ziemba, L., and Zuidema, P.: Aerosol–Cloud–Meteorology Interaction Airborne Field Investigations: Using Lessons Learned from the U.S. West Coast in the Design of ACTIVATE off the U.S. East

Coast, Bulletin of the American Meteorological Society, 100(8), 1511 - 1528 , https://doi.org/10.1175/BAMS-D-18-0100.1, 2019.

Stamnes, S., Hostetler, C., Ferrare, R., Burton, S., Liu, X., Hair, J., Hu, Y., Wasilewski, A., Martin, W., van Diedenhoven, B., Chowdhary, J., Cetinic, I., Berg, L. K., Stamnes, K., and Cairns, B.: Simultaneous polarimeter retrievals of microphysical aerosol and ocean color parameters from the MAPP algorithm with comparison to high-spectral-resolution lidar aerosol and ocean products, Appl. Optics, 57(10), 2394--2413 , https://doi.org/10.1364/AO.57.002394, 2018.

Stone, L. D.: Theory of optimal search (2nd edition), INFORMS, ISBN 1-877640-00-X, 1989.

Thompson, D. R., Guanter, L., Berk, A., Gao, B.-C., Richter, R., Schläpfer, D., and Thome, K. J.: Retrieval of Atmospheric Parameters and Surface Reflectance from Visible and Shortwave Infrared Imaging Spectroscopy Data, Surveys in Geophysics, 40(3), 333--360, https://doi.org/10.1007/s10712-018-9488-9, 2019.

Thompson, D. R., Braverman, A., Brodrick, P. G., Candela, A., Carmon, N., Clark, R. N., Connelly, D., Green, R. O., Kokaly, R. F., Li, L., Mahowald, N., Miller, R. L., Okin, G. S., Painter, T. H., Swayze, G. A., Turmon, M., Susilouto, J., and Wettergreen, D. S.: Quantifying uncertainty for remote spectroscopy of surface composition, Remote Sensing of Environment, 247, 111898 , https://doi.org/https://doi.org/10.1016/j.rse.2020.111898, 2020.

Thorpe, A. K., Frankenberg, C., Thompson, D. R., Duren, R. M., Aubrey, A. D., Bue, B. D., Green, R. O., Gerilowski, K., Krings, T., Borchardt, J., Kort, E. A., Sweeney, C., Conley, S., Roberts, D. A., and Dennison, P. E.: Airborne DOAS retrievals of methane, carbon dioxide, and water vapor concentrations at high spatial resolution: application to AVIRIS-NG, Atmos. Meas. Tech., 10, 3833–3850, https://doi.org/10.5194/amt-10-3833-2017, 2017.

Torres, O., Tanskanen, A., Veihelmann, B., Ahn, C., Braak, R., Bhartia, P. K., Veefkind, P., and Levelt, P.: Aerosols and surface UV products from Ozone Monitoring Instrument observations: An overview, J. Geophys. Res, 112(D24), D24S47, 2007.

Vane, G., Green, R. O., Chrien, T. G., Enmark, H. T., Hansen, E. G., and Porter, W. M.: The airborne visible/infrared imaging spectrometer (AVIRIS), Remote Sensing of Environment, 44(2), 127-143, https://doi.org/https://doi.org/10.1016/0034-4257(93)90012-M, 1993.

Virtanen, T. H., Kolmonen, P., Sogacheva, L., Rodriguez, E., Saponaro, G., and de Leeuw, G.: Collocation mismatch uncertainties in satellite aerosol retrieval validation, Atmos. Meas. Tech., 11, 925–938. https://doi.org/10.5194/amt-11-925-2018, 2018.

Volz, F. E. (1959), Photometer mit Selen-photoelement zurs- pektralen Messung der Sonnenstrahlung und zer Bestim- mung der Wallenlangenabhangigkeit der Dunsttrubung. Arch. Meteorol. Geophys. Bioklim. B10:100–131.

Wang, M. and Bailey, S. W.: Correction of sun glint contamination on the SeaWiFS ocean and atmosphere products, Appl. Optics, 40(27), 4790--4798, 2001.

Waquet, F., Cairns, B., Knobelspiesse, K., Chowdhary, J., Travis, L., Schmid, B., and Mishchenko, M.: Polarimetric remote sensing of aerosols over land, J. Geophys. Res, 114, 2009.

Weiss, J. R., Smythe, W. D., and Wenwen Lu: Science traceability. in: 2005 IEEE Aerospace Conference 292-299), https://doi.org/10.1109/AERO.2005.1559323, 2005.

Winker, D. M., Vaughan, M. A., Omar, A., Hu, Y., Powell, K. A., Liu, Z., Hunt, W. H., and Young, S. A.: Overview of the CALIPSO mission and CALIOP data processing algorithms, J. Atmos. Ocean Tech., 26(11), 2310--2323, 2009.

Xu, F., Harten, G., Diner, D. J., Davis, A. B., Seidel, F. C., Rheingans, B., Tosca, M., Alexandrov, M. D., Cairns, B., Ferrare, R. A., Burton, S. P., Fenn, M. A., Hostetler, C. A., Wood, R., and Redemann, J.: Coupled Retrieval of Liquid Water Cloud and Above-Cloud Aerosol Properties Using the Airborne Multiangle SpectroPolarimetric Imager (AirMSPI), J. Geophys. Res-Atmos., 123, 3175-3204, https://doi.org/10.1002/2017JD027926, 2018.

Xu, F., Diner, D. J., Dubovik, O., and Schechner, Y.: A Correlated Multi-Pixel Inversion Approach for Aerosol Remote Sensing, Remote Sensing, 11(7), https://doi.org/10.3390/rs11070746, 2019.

Xu, F., Gao, L., Redemann, J., Flynn, C. J., Espinosa, W. R., da Silva, A. M., Stamnes, S., Burton, S. P., Liu, X., Ferrare, R., Cairns, B., and Dubovik, O.: A Combined Lidar-Polarimeter Inversion Approach for Aerosol Remote Sensing Over Ocean, Frontiers in Remote Sensing, 2, 2, https://doi.org/10.3389/frsen.2021.620871, 2021.

Yin, Z., Ansmann, A., Baars, H., Seifert, P., Engelmann, R., Radenz, M., Jimenez, C., Herzog, A., Ohneiser, K., Hanbuch, K., Blarel, L., Goloub, P., Dubois, G., Victori, S., and Maupin, F.: Aerosol measurements with a shipborne Sun--sky--lunar photometer and collocated multiwavelength Raman polarization lidar over the Atlantic Ocean, Atmospheric Measurement Techniques, 12(10), 5685--5698 , https://doi.org/10.5194/amt-12-5685-2019, 2019.

Yorks, J. E., Hlavka, D. L., Vaughan, M. A., McGill, M. J., Hart, W. D., Rodier, S., and Kuehn, R.: Airborne validation of cirrus cloud properties derived from CALIPSO lidar measurements: Spatial properties, J. Geophys. Res-Atmos., 116(D19), 2011.

Yorks, J. E., McGill, M. J., Palm, S. P., Hlavka, D. L., Selmer, P. A., Nowottnick, E. P., Vaughan, M. A., Rodier, S. D., and Hart, W. D.: An overview of the CATS level 1 processing algorithms and data products, Geophys. Res. Lett., 43(9), 4632-4639, https://doi.org/10.1002/2016GL068006, 2016.

Zibordi, G., Mélin, F., Berthon, J.-F., Holben, B., Slutsker, I., Giles, D., D'Alimonte, D., Vandemark, D., Feng, H., Schuster, G., Fabbri, B. E., Kaitala, S., and Seppälä, J.: AERONET-OC: A Network for the Validation of Ocean Color Primary Products, J. Atmos. Ocean Tech., 26(8), 1634-1651, https://doi.org/10.1175/2009JTECHO654.1, 2009.

Zibordi, G., Holben, B., Mélin, F., D'Alimonte, D., Berthon, J. F., Slutsker, I., and Giles, D.: AERONET-OC: an overview, Canadian Journal of Remote Sensing, 36(5), 488--497, 2010.

Zibordi, G., Mélin, F.: An evaluation of marine regions relevant for ocean color system vicarious calibration. Remote Sens. Environ. 190, 122–136. https://doi.org/10.1016/J.RSE.2016.11.020, 2017.